© 2018. Published by The Company of Biologists Ltd | Development (2018) 145, dev170639. doi:10.1242/dev.170639

STEM CELLS AND REGENERATION

RESEARCH ARTICLE

Drosophila small ovary gene is required for transposon silencing and heterochromatin organization, and ensures germline stem cell maintenance and differentiation

Ferenc Jankovics[1,*], Melinda Bence[1], Rita Sinka[2], Anikó Faragó[3], László Bodai[3], Aladár Pettkó-Szandtner[4], Karam Ibrahim[1], Zsanett Takács[1], Alexandra Brigitta Szarka-Kovács[1] and Miklós Erdélyi[1,*]

ABSTRACT

Self-renewal and differentiation of stem cells is one of the fundamental biological phenomena relying on proper chromatin organization. In our study, we describe a novel chromatin regulator encoded by the *Drosophila small ovary* (*sov*) gene. We demonstrate that *sov* is required in both the germline stem cells (GSCs) and the surrounding somatic niche cells to ensure GSC survival and differentiation. *sov* maintains niche integrity and function by repressing transposon mobility, not only in the germline, but also in the soma. Protein interactome analysis of Sov revealed an interaction between Sov and HP1a. In the germ cell nuclei, Sov colocalizes with HP1a, suggesting that Sov affects transposon repression as a component of the heterochromatin. In a position-effect variegation assay, we found a dominant genetic interaction between *sov* and HP1a, indicating their functional cooperation in promoting the spread of heterochromatin. An *in vivo* tethering assay and FRAP analysis revealed that Sov enhances heterochromatin formation by supporting the recruitment of HP1a to the chromatin. We propose a model in which *sov* maintains GSC niche integrity by regulating transposon silencing and heterochromatin formation.

KEY WORDS: *Drosophila*, Stem cell niche, piRNA, Chromatin, Heterochromatin, HP1a

INTRODUCTION

The eukaryotic genome is organized into structurally distinct and functionally specialized chromatin domains, called euchromatin and heterochromatin (Heitz, 1928). The euchromatic domain contains actively transcribed genes, whereas the heterochromatin is mainly associated with a repressive transcriptional state (Wang et al., 2016). The heterochromatin is enriched in repetitive elements and transposons that occupy the centromeric and telomeric regions of the chromosomes (Brutlag et al., 1978; Peacock et al., 1978). Another domain of the heterochromatin is formed at regulatory regions of genes that have to be transcriptionally repressed at specific stages of development. The heterochromatin is epigenetically defined by a combination of specific covalent modifications of histone molecules. The formation of the heterochromatin is accompanied by trimethylation of Histone 3 at Lysine 9 (H3K9me3), which recruits Heterochromatin protein 1a [HP1a, encoded by *Su(var)205*] initiating the formation of the repressive chromatin environment (Bannister et al., 2001; Rea et al., 2000). Heterochromatic domains are organized around HP1a into phase-separated liquid compartments that physically compact chromatin and recruit additional repressive components (Larson et al., 2017; Strom et al., 2017). Kinetic analysis of HP1-chromatin binding revealed a complex interaction between heterochromatin components; however, the precise molecular mechanisms required for formation and maintenance of heterochromatin domains are not completely understood (Bryan et al., 2017).

In eukaryotes, a heterochromatin-dependent, small non-coding RNA-based defence system has been evolved against transposon-induced mutagenesis (Tóth et al., 2016). Central components of this pathway are the Piwi-interacting RNAs (piRNAs). Long precursors of the piRNAs are transcribed from both uni-strand and dual-strand piRNA clusters containing transposon sequences (Brennecke et al., 2007). Following piRNA biogenesis in the cytoplasm, mature short piRNAs associate with members of the Piwi class of the Argonaute protein superfamily (Piwi, Aub and Ago3 in *Drosophila*) and form RISC complexes (Huang et al., 2017). In the germ cells, Aub- and Ago3-RISC complexes mediate the post-transcriptional silencing of the transposons by inducing the degradation of transposon transcripts in the cytoplasm. The Piwi-RISC complex, however, migrates into the nucleus and inhibits transposon transcription. In the somatic cells of the ovary, exclusively the Piwi-RISC-mediated transcriptional silencing inhibits transposon activity (Le Thomas et al., 2013; Malone et al., 2009).

Two steps of the piRNA pathway have been shown to depend on heterochromatin function (Sato and Siomi, 2018). First, long precursors of the piRNAs are transcribed from piRNA clusters located mainly at the heterochromatic regions of the genome. Disruption of heterochromatin formation by *eggless/dSetdb1* (*egg*) or *Su(var)205* mutations impedes the transcription of the clusters, which results in derepression of transposons (Rangan et al., 2011; Teo et al., 2018). The second heterochromatin-dependent step of the piRNA pathway is the transcriptional silencing of the transposon transcription. At the transposon loci, Piwi-RISC inhibits transposon transcription by inducing the formation of a repressive heterochromatic environment on the transposon loci (Le Thomas et al., 2013). Transcriptional silencing of the transposons includes the deposition of repressive H3K9me3 modification mark and the recruitment of HP1a to the chromatin of the transposon locus.

Drosophila oogenesis provides an excellent model for understanding mechanisms of heterochromatin formation and its

[1]Institute of Genetics, Biological Research Centre of the Hungarian Academy of Sciences, Szeged 6726, Hungary. [2]Department of Genetics, University of Szeged, Szeged 6726, Hungary. [3]Department of Biochemistry and Molecular Biology, University of Szeged, Szeged 6726, Hungary. [4]Laboratory of Proteomics Research, Biological Research Centre of the Hungarian Academy of Sciences, Szeged 6726, Hungary.

*Authors for correspondence (erdelyi.miklos@brc.mta.hu; jankovics.ferenc@brc.mta.hu)

F.J., 0000-0001-9697-4472; M.E., 0000-0002-9501-5752

Received 6 August 2018; Accepted 29 October 2018

Development (2018) 145, dev170639. doi:10.1242/dev.170639

function in gene expression regulation and transposon silencing. In the ovary, repeated divisions of germline stem cells (GSCs) ensures continuous production of germ cells (Eliazer and Buszczak, 2011). GSCs reside stem cell niches, which are located in the germaria at the anterior tip of the ovary (Lin and Spradling, 1993). The GSC niches are composed of three somatic cell types, terminal filament cells, cap cells and escort cells (ECs), which provide physical and signalling milieu required for GSC self-renewal and differentiation (Fig. 1A) (Chen et al., 2011). Mitotic division of the GSC reproduces the GSC and generates a committed progenitor cell, the so-called cystoblast. The cystoblast has a limited division capacity and generates 16 interconnected cyst cells. One of the cyst cells differentiates into an oocyte whereas the remaining 15 cyst cells become supportive nurse cells. The developing germ cells are surrounded by an epithelial monolayer of somatic follicle cells forming an egg chamber.

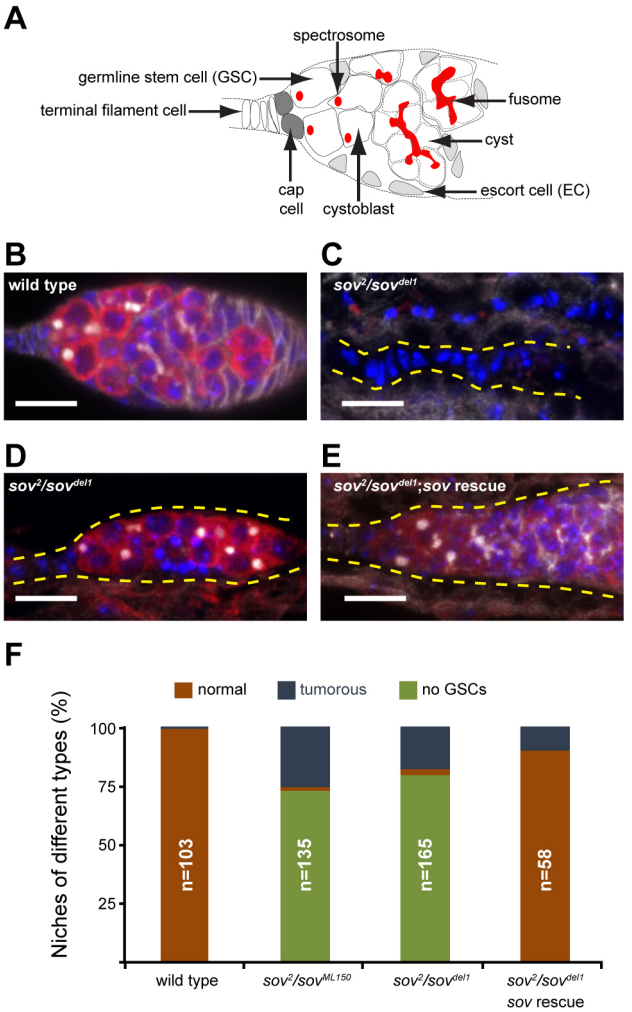

Fig. 1. Sov mutations lead to GSC loss and formation of tumours. (A) The cellular composition of the germarium. (B-D) Immunostaining of a wild-type germarium (B) and a sov^{2}/sov^{del1} germarium (C,D) with GSC loss (C) and a germ cell tumour (D). (E) Rescue of the niche defects in a sov^{2}/sov^{del1}; *Dp(1;2)FF184439* germarium. Spectrosomes and fusomes are labelled with HTS (white), germ cells are labelled for Vasa (red); DAPI is blue. Yellow dashed lines outline the mutant germaria. Scale bars: 10 µm. (F) Quantification of the *sov* mutant phenotypes. The lack of GSCs in the mutants can be rescued.

In a previous RNAi-based screen for genes regulating germ cell behaviour, we have identified several essential chromatin regulators, such as *Su(var)205* and *Su(var)2-10*, to be involved in germ cell development (Jankovics et al., 2014). In the same screen, we identified the annotated *CG14438* gene, which has been shown to be involved in transposon silencing and to co-immunoprecipitate with HP1a (Alekseyenko et al., 2014; Czech et al., 2013; Muerdter et al., 2013). To gain a better understanding of chromatin regulation during germ cell development, we analysed the function of *CG14438* in *Drosophila* oogenesis. Here, we show that *CG14438* is identical to *small ovary* (*sov*) gene and it is a novel chromatin regulator that promotes heterochromatin formation by stabilizing the association of HP1a with the chromatin. Our results suggest that Sov suppresses transposon activity by regulating the transcription of the dual-stranded piRNA clusters and by the transcriptional silencing of the transposons. In the stem cell niche, *sov* function is required both in the somatic and in the germ cells to ensure GSC maintenance and differentiation.

RESULTS

CG11438 and *small ovary* (*sov*) are identical

CG14438 encodes a single large protein of 3313 amino acids (Fig. S1A). The N-terminal half of the protein is highly unstructured and contains a putative intrinsically disordered RGG/RG domain mediating degenerate specificity in RNA binding (Ozdilek et al., 2017; Thandapani et al., 2013). The C-terminal half of the protein contains 21 zinc-finger domains and a PxVxL pentamer motif, which is a canonical HP1-binding domain (Smothers and Henikoff, 2000).

We generated a null allele of *CG14438*, which removes the entire coding region of the gene (Fig. S1B). Animals homozygous for the novel deletion allele, which we called $CG14438^{del1}$, died at the third larval stage, indicating that *CG14438* is an essential gene. Complementation analysis between $CG14438^{del1}$ and alleles of genes mapping to the same genomic region revealed that $CG14438^{del1}$ does not complement alleles of *sov* (Wayne et al., 1995).

To confirm that *CG14438* corresponds to *sov*, we performed a series of rescue experiments. The Dp(1;3)DC486 duplication, which covers a 92.5 kb genomic region around the *CG14438/sov* locus, rescued all *sov* phenotypes, indicating that the *sov* gene is localized in this genomic region. Identical rescue was observed with two overlapping genomic transgenes [Dp(1;2)FF026056 and Dp(1;3)FF184439] (Fig. S1B). Sequencing of the sov^{2} allele revealed a point mutation in the *CG14438*-coding region generating a premature stop codon after amino acid 3151 that results in a truncated mutant protein lacking 152 C-terminal amino acids (Fig. S1A). Taken together, the complementation analysis, the rescue experiments and the sequencing of the *sov* mutant allele indicate that CG14438 and *sov* are identical.

Sov is required for GSC maintenance and differentiation

sov is an essential gene but its hypomorphic allelic combinations result in similar ovarian morphology to that of *CG14438* RNAi (Jankovics et al., 2014; Wayne et al., 1995). To gain insights into the function of *sov* in germ cell development, we made use of the hypomorphic allelic combinations sov^{2}/sov^{ML150} and sov^{2}/sov^{del1}. Females were sterile and exhibited rudimentary ovaries. In most of the germaria, no germ cells were found, indicating a role for *sov* in germ cell maintenance (Fig. 1C,F). In addition to the agametic germaria, ~30% of the mutant germaria exhibited germ cell tumours (Fig. 1D,F). Each tumour cell contained a single spectrosome, a hallmark of the GSC or cystoblast-like undifferentiated germ cells, indicating that *sov* is required not only for GSC maintenance but also

Development (2018) 145, dev170639. doi:10.1242/dev.170639

for GSC differentiation. The GSC maintenance and differentiation defects were rescued by the Dp(1;3)FF184439 transgene expressing the *sov* gene from its genomic context (Fig. 1E,F).

sov is required cell-autonomously for GSC maintenance at the adult stage

To narrow the temporal and spatial requirement of *sov* in germ cell development, tissue-specific RNAi and clonal analysis were performed. Silencing of *sov* with the germline-specific nosGal4 driver caused female sterility. Young females possessed normal-looking ovaries (Fig. 2B,D) and laid eggs that did not hatch. However, depletion of *sov* in the germ line resulted in a progressive loss of GSCs. In 4-week old sovRNAi females, most of the niches lost the GSCs and contained no germ cells, indicating that *sov* is required cell-autonomously in the germ line for GSC maintenance (Fig. 2C,D).

A cell-autonomous requirement for *sov* in germ cell maintenance was confirmed by analysis of *sov* mutant germline clones. Homozygous mutant sov^{del1} germ cells were induced by FLP/FRT-mediated recombination and identified by the lack of the GFP marker gene (Fig. S2A,B). To analyse *sov* function at the larval stage, *sov* mutant germ line clones were induced in L1 larvae and the phenotype was analysed in adults. In 3-day-old females, GSCs were found in the *sov* mutants similar to the wild-type clones, indicating that *sov* mutant larval germ cells can populate the niche and can develop into normal GSCs (Fig. S2C). This indicates that *sov* function is dispensable in the germ line between L1 and the adult stage. To analyse *sov* function specifically in adult GSCs, clones were induced in the germ cells of young females. Both in the control and in the mutant niches, GFP-minus GSCs appeared in the first week after clone induction (ACI) (Fig. S2D). Wild-type control clones were maintained even later than 4 weeks ACI; however, the number of niches carrying *sov* mutant GSCs decreased (Fig. S2D).

Taken together, our data show that *sov* is required for GSC maintenance intrinsically in the germline at the adult stage. Remarkably, loss of *sov* in the GSCs located in niches composed of wild-type somatic cells did not induce tumour formation, indicating that the differentiation defect observed in *sov* mutants is not germ-cell-autonomous.

Sov is required in ECs for GSC maintenance, germ cell differentiation and EC survival

Formation of tumours composed of undifferentiated GSC-like cells and GSC loss could be a consequence of defects in the somatic cells of the niche. Depending on their position in the germarium, ECs have two distinct functions (Wang and Page-McCaw, 2018). Anterior ECs promote GSC self-renewal and maintain GSCs in stem cell state. Posterior ECs, however, promote GSC differentiation. Thus, loss of ECs in *sov* mutants results in a dual phenotype: GSC loss if the anterior ECs are lost, or a GSC tumour, if the posterior ECs die. In *sov* mutant niches, the number of the ECs was reduced, indicating that *sov* is required for EC survival (Fig. 3B,E). Consistent with the EC loss, we observed accumulation of activated Caspase3 in the *sov* mutant niches (Fig. S3). A similar reduction in EC numbers was observed when *sov* was silenced specifically in the somatic cells by the c587Gal4 driver, indicating that the requirement of *sov* for EC survival is cell autonomous (Fig. 3C,D,E).

Next, we investigated how somatic *sov* function affects germline behaviour. Therefore, the c587Gal4 line was used to induce *sov* silencing in the ECs and the germ cells were analysed. Silencing of *sov* in the ECs induced GSC loss and formation of GSC-like tumours in the niches (Fig. 3C,D,F). This indicates that *sov* is required in the ECs in a non-cell-autonomous manner for GSC maintenance and differentiation.

This *sov* RNAi phenotype in GSCs could be a consequence of earlier defects induced in the larval ancestors of the ECs. To induce adult-specific *sov* silencing in the ECs, the temperature-sensitive $Gal80^{ts}$ mutant was used. At the permissive temperature (18°C), *sov* is not silenced in *c587Gal4;sovRNAi;*$Gal80^{ts}$ flies and no abnormalities are detectable in the niche (Fig. 3F). However, shifting the adult females to the restrictive temperature (29°C) allowed Gal4-driven *sov* silencing in the ECs that, in turn, resulted in germline defects similar to those of *sov* mutants. Two weeks after RNAi induction, germ cell tumours were formed and GSCs were lost (Fig. 3F).

Homozygous EC clones were induced in L1 larvae or in 1-day-old adult females, and the numbers of germaria containing homozygous *sov* mutant and wild-type EC clones were determined in 4-day-old females (Fig. S4A,B). The frequency of germaria containing *sov* mutant ECs was reduced compared with wild-type clone frequency (Fig. S4C). These germaria contained fewer *sov* mutant ECs, confirming the results obtained by analysis of mutant allelic combinations and the RNAi data on the requirement of *sov* in EC survival (Fig. S4D).

In summary, *sov* is required for EC survival in the adult niches, which ensures GSC differentiation and maintenance in a non-cell-autonomous manner.

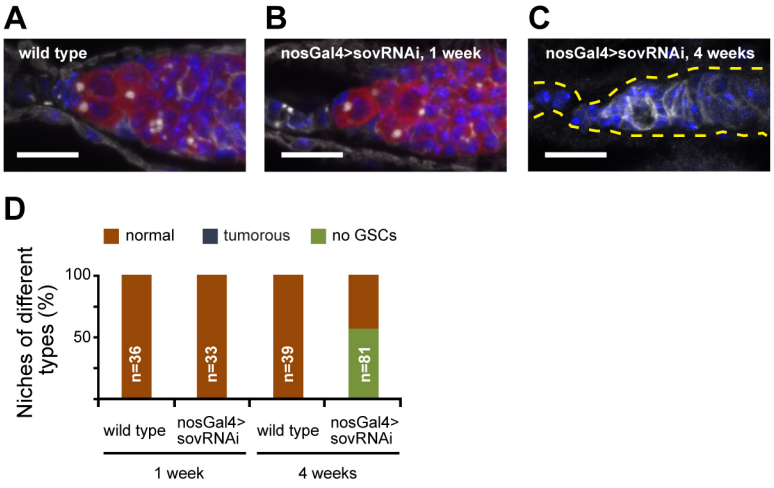

Fig. 2. Sov is required cell-autonomously for GSC maintenance. (A-D) Germline-specific *sov* silencing. Immunostaining of a wild-type germarium (A), and germaria of a 1-week-old (B) and a 4-week-old (C) *nosGal4>sovRNAi* females. The 4-week-old germaria lack germ cells. Yellow dashed lines outline the abnormal germarium in C. Spectrosomes and fusomes are labelled with HTS (white), germ cells are labelled for Vasa (red); DAPI is blue. Scale bars: 10 µm. (D) Quantification of the phenotypes induced by germline-specific *sov* silencing. Sov-silenced GSCs are progressively lost from the niche.

Development (2018) 145, dev170639. doi:10.1242/dev.170639

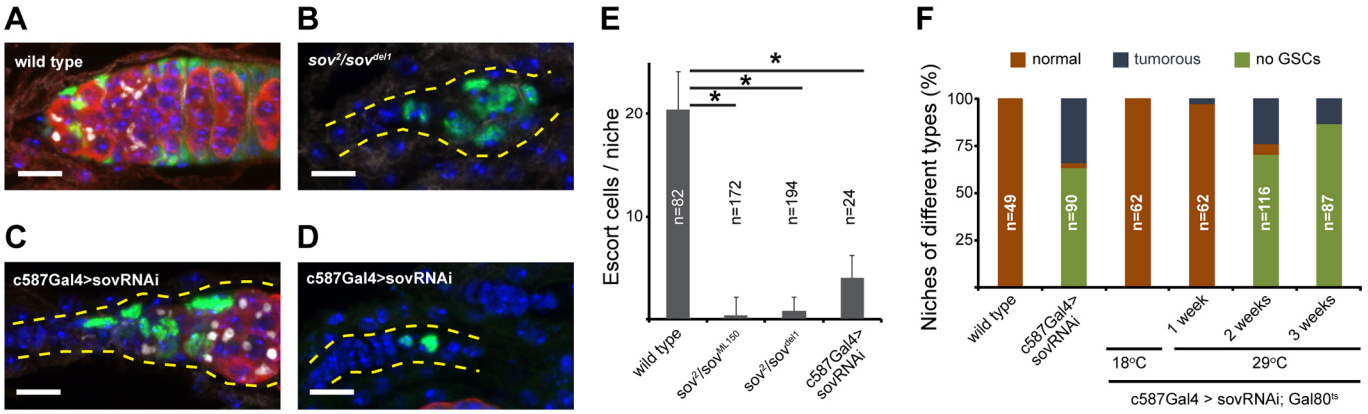

Fig. 3. Sov is required in ECs for GSC maintenance, germ cell differentiation and EC survival. (A-D) Immunostaining of a wild-type germarium (A) and a *sov*^{2}/*sov*^{del1} germarium with reduced EC number (B). Immunostaining of *c587Gal4>sovRNAi* germaria with reduced EC number and exhibiting germ cell tumour (C) and GSC-loss (D) phenotypes. Yellow dashed lines outline the abnormal germaria. Spectrosomes and fusomes are labelled with HTS (white), germ cells are labelled for Vasa (red), ECs are labelled for Traffic jam (Tj) (green); DAPI is blue. Scale bars: 10 µm. (E) Quantification of EC number in *sov* mutant and *c587Gal4>sovRNAi* niches. Loss of *sov* in the ECs leads to the loss of ECs from the niche. Data are mean±s.d.; *t*-test, **P*<0.05. (F) Quantification of the mutant niche phenotypes. Loss of *sov* in the ECs leads to the loss of GSCs and to the formation of GSC-like tumours in the niches.

Sov promotes GSC differentiation by restricting Dpp-signalling activity in the niche

In the niche, a complex regulatory network controls GSC differentiation. To explore further the function of *sov* in GSC differentiation, we analysed the activity of the signalling pathways involved in communication between different cell types of the niche.

In GSCs, the repression of *bam* expression prevents differentiation of the stem cells (McKearin and Ohlstein, 1995). In the wild type, *bam* expression is initiated in the GSC daughter cells that lose physical contact with the cap cells and adopt cystoblast fate. In *sov* mutant germaria, no *bam* expression was detected when monitored with the reporter line *bam*-GFP (Fig. S5A,B). Forced expression of *bam* from the heat shock-inducible hs-*bam* transgene was sufficient to induce differentiation of the *sov* mutant germ cells, as indicated by the formation of fusome containing cysts and an almost complete lack of GSC-like tumours in the *sov*^{2}/*sov*^{ML150}; *hs-bam* females (Fig. S5C-E). Based on these data, we conclude that *sov* acts upstream of *bam* in the GSC differentiation process.

In the niche, the primary factor that represses *bam* expression in the GSCs is Dpp, the *Drosophila* TGFβ homolog (Song et al., 2004). In the wild type, Dpp activity is restricted to the GSCs and can be monitored by the nuclear translocation of pMad. Sov mutant tumour cells located outside the GSC niche accumulate pMad in their nuclei, indicating that expanded Dpp activity is responsible for the maintenance of *bam* repression in the *sov* mutant germ cells (Fig. S5F,G).

Restriction of Dpp activity to the GSCs can be adjusted by controlled diffusion of the secreted Dpp ligand. In wild-type germaria, ECs extend long cellular protrusions that enwrap differentiating GSC daughter cells, separating them from the Dpp signal (Fig. S5H). Sov mutant ECs, however, fail to extend protrusions, indicating that *sov* controls the accessibility of the secreted Dpp (Fig. S5I). Niche abnormalities caused by the lack of EC protrusions resemble the phenotypes that have been observed in niches with impaired Wnt4 function (Mottier-Pavie et al., 2016; Upadhyay et al., 2016). To test the involvement of *sov* in Wnt4-mediated niche regulation, Wnt4 expression was analysed in *sov* mutants. RT-qPCR revealed that Wnt4 mRNA levels were reduced in *sov* mutant niches, indicating that *sov* is required for Wnt4 expression (Fig. S5J). Forced expression of Wnt4 in *sov* RNAi ECs by two different transgenic constructs, however, did not rescue the germ cell differentiation defects caused by *sov* silencing, indicating that *sov* regulates GSC development not exclusively by promoting Wnt4 expression (Fig. S5K). Taken together, *sov* promotes protrusion formation in the ECs that separates the GSC daughter cell from the Dpp source and enables its Bam-driven differentiation.

Sov is required in both somatic and germline cells for transposon repression

Remarkably, GSC and EC defects of *sov* mutants resemble that of *egg*, *HP1a* or *piwi*, which are essential regulators of heterochromatin formation and transposon repression in *Drosophila* (Jin et al., 2013; Ma et al., 2014; Rangan et al., 2011; Wang et al., 2011). Thus, we hypothesized that Sov regulates niche integrity by suppressing transposon activity via heterochromatin regulation.

Transposons can be classified into three groups depending on whether they are predominantly expressed in the germline cells (e.g. *HET-A* and *Burdock*), in somatic cells (e.g. *gypsy*) or in both cell types (Malone et al., 2009). Therefore, we used transposon sensors, RT-qPCR and RNA-seq to analyse the expression of specific transposons in ovaries silenced for *sov* specifically in the germ cells or in the soma.

Transposon sensors contain transposon-derived sequences that are targeted by the piRNAs, resulting in repression of the *LacZ* reporter gene. First, we used sensors for the germline-dominant *HET-A* and the *Burdock* transposons (Dönertas et al., 2013). The MTD-Gal4 driver was used to drive the germline-specific expression of three independent *sov* RNAi lines. In all *MTDGal4>sovRNAi* ovaries, a robust β-galactosidase (β-Gal) expression was detected from both transposon sensors, suggesting derepression of transposons (Fig. 4A-D). Consistent with these results, a strong accumulation of the endogenous germline-dominant *HET-A* and *Burdock* transposon mRNA levels was detected in *nosGal4>sovRNAi* ovaries using RT-qPCR (Fig. 4I). To determine the germ line-specific effect of *sov* on the steady-state RNA levels of all transposon classes, polyA-RNAs were sequenced from *nosGal4>sovRNAi* and *nosGal4>wRNAi* control ovaries (RNA-seq). In the *nosGal4>sovRNAi* ovaries, a robust upregulation of transcript levels for all germ-line dominant transposons was detected, indicating that *sov* is required for repression of transposon activity in the germline (Fig. 4J).

To analyse the effect of *sov* on transposon silencing in the soma, we made use of the *gypsy*-LacZ transposon sensor, which reflects

Development (2018) 145, dev170639. doi:10.1242/dev.170639

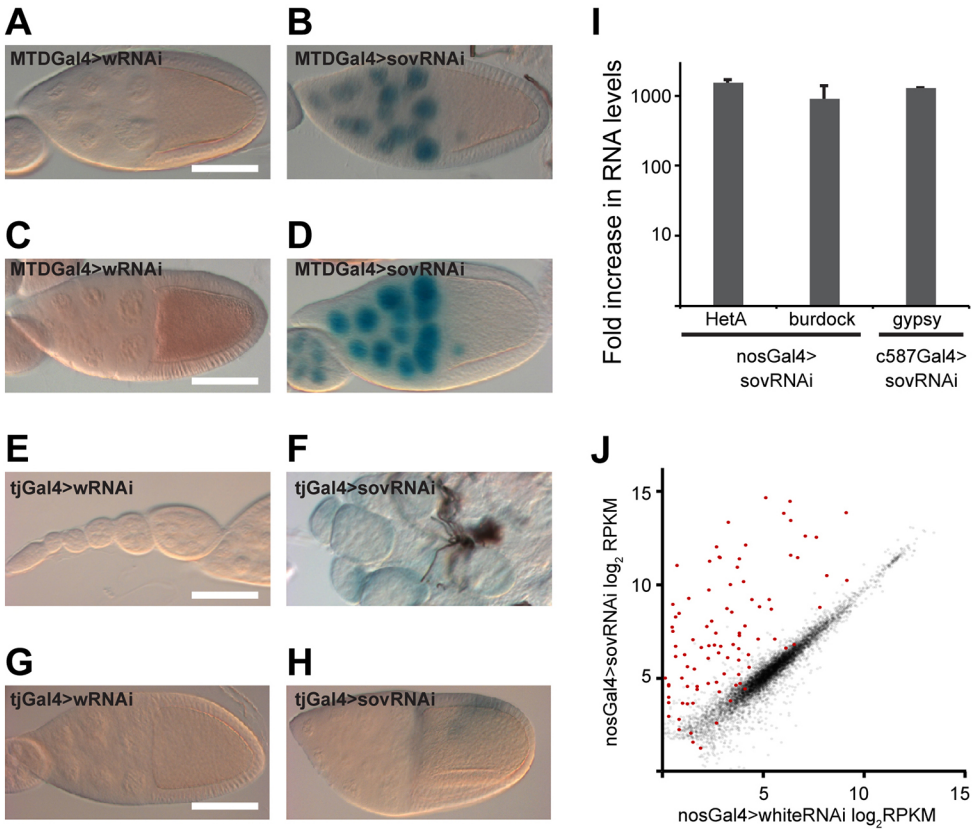

Fig. 4. Sov is required in both somatic and germline cells for transposon repression. (A-H) β-Gal staining of wild-type and *sov*-silenced egg chambers expressing *HeT-A* (A,B), *Burdock* (C,D), *gypsy* (E-H) reporters. For *sov* silencing, TRiP-HMC04875 (H) and 3-2 (B,D,F) was used. Scale bars: 50 µm. (I) Fold changes in steady-state mRNA levels of indicated transposons measured by RT-qPCR are shown. (J) Scatter plot showing expression levels of genes (grey) in *nosGal4>sovRNAi* ovaries. Transposons are in shown in red.

the expression of the soma-dominant *gypsy* transposon (Dönertas et al., 2013). Somatic silencing of *sov* with the 3-2 and KK103679 RNAi lines resulted in severe morphological abnormalities of the ovaries, which made the analysis of the *gypsy-LacZ* reporter difficult. Nevertheless, we detected a strong β-Gal accumulation by Tj-Gal4-driven expression of the silencing constructs, indicating transposon derepression by *sov* silencing (Fig. 4E,F). Somatic silencing of *sov* with the weak HMC04875 RNAi line resulted in the formation of normal egg chambers with normal-looking somatic cells and the oogenesis was completed. Despite the modest phenotypic consequences of *sov* silencing by this RNAi construct, a weak β-Gal expression was detected in the somatic cells (Fig. 4G,H). Results obtained through analysis of the *gypsy*-LacZ transposon sensor were confirmed by measuring endogenous *gypsy* mRNA levels in the *sov*-silenced ovaries. RT-qPCR on c587Gal4>*sovRNAi* ovaries revealed a robust accumulation of the endogenous *gypsy* mRNAs, indicating that *sov* functions in the repression of the somatic transposon activity (Fig. 4I).

In summary, derepression of the reporter expression from the sensors and upregulation of the endogenous transposons by impaired *sov* function revealed an essential role for *sov* in transposon repression, both in the germline and in the soma.

Loss of *sov* induces DNA damage, abnormal axis specification and apoptosis in the germ line

Derepression of transposons results in accumulation of double-stranded breaks (DSBs) on the chromosomes, which are recognized by the histone variant γH2Av. In the wild type, γH2Av accumulates in nuclei of germ cells in the 16 cell cysts undergoing meiotic recombination in region 2 of the germaria. As meiosis is accomplished, meiotic DSBs are repaired and γH2Av levels are reduced in the wild-type germ cells (Fig. S6A,C). In contrast, an overall high level of γH2Av was detected in the nuclei of *sov* RNAi germ cells prior and after meiosis (Fig. S6B,D). Accumulation of γH2Av was initiated in the GSCs, indicating the formation of DSBs, presumably caused by transposon mobilization.

Transposon-induced DNA damage has been shown to activate the Chk2-dependent checkpoint (Chen et al., 2007; Klattenhoff et al., 2007). Activation of the Chk2 and ATR kinases induces microtubule organization defects in the oocytes, which lead to Gurken (*grk*), *oskar* RNA (*osk*) and Vasa delocalization and, thus, abnormal axis specification (Abdu et al., 2002; Ghabrial and Schüpbach, 1999). In *sov* RNAi germ cells, no Vasa was detected at the posterior pole of the oocytes, indicating a disrupted AP polarity (Fig. S6E,F). Prior to Vasa, *osk* mRNA is localized to the posterior pole of the wild-type oocytes where it is translated. However, neither *osk* mRNA (Fig. S6G,H) nor Osk protein (Fig. S6E,F) accumulation was detected at the posterior of *sov*-depleted oocytes. In addition, no anterodorsal localization of Grk was detected in *sov* RNAi oocytes (Fig. S6E,F). Consistent with the lack of Grk localization, all eggs laid by *nosGal4>sovRNAi* females exhibited severe ventralized eggshell-patterning defects with fused or absent dorsal appendages (Fig. S6I,J). Analysis of the RNA-seq data revealed an increased expression of the apoptotic genes *hid* and *reaper* in the *sov* RNAi germ cells, suggesting that loss of Sov induces apoptosis (Fig. S6K). Taken together, our data indicate that loss of *sov* function in the germ line results in transposon derepression, which, in turn, leads to DNA damage, abnormal axis specification and apoptosis.

Sov promotes heterochromatin formation by stabilization of heterochromatic domains

To identify the mechanisms by which Sov regulates transposon repression, we first determined the subcellular localization of

Development (2018) 145, dev170639. doi:10.1242/dev.170639

GFP-tagged Sov expressed from a genomic fosmid construct. The tagged Sov variant completely rescued the sterile and the lethal phenotypes associated with *sov* mutations. In sov^{del1}; *Sov:GFP* females, we detected ubiquitous Sov expression in the somatic and germ cells of the ovary. Sov localized in the nuclei and accumulated at nuclear foci (Fig. 5A). At these foci, Sov partially colocalized with HP1a and Centrosome identifier (Cid), suggesting a direct role for Sov in chromatin regulation (Fig. 5B,C).

To identify Sov interacting proteins, we affinity purified Sov from the sov^{del1}; *Sov:GFP* ovaries on six independent occasions and performed mass spectrometry (LC-MS/MS) analysis of the samples. Consistent with the colocalization in the nuclei, Sov co-immunoprecipitated with HP1a, indicating that *sov* affects transposon repression as a chromatin regulator (Fig. 5D). This role of Sov was confirmed in a pericentromeric position effect variegation (PEV) assay. For the assay, the w^{m4h} allele was used, in which the *white* gene responsible for the red eye colour is translocated to the border between the pericentromeric heterochromatin and the euchromatin. In the individual facets of the compound fly eye, stochastic spreading of the heterochromatin permits or inhibits expression of the white gene, leading to a variegating eye colour (Elgin and Reuter, 2013).

In heterozygous sov^{ML150} and sov^{del1} flies, we detected increased eye pigment production, indicating a dominant suppressor effect of *sov* on PEV (Fig. 5E). Dominant PEV-suppression of the w^{m4h} allele suggests that Sov promotes heterochromatin formation at the pericentromeric regions of the genome. The positive effect of *sov* on heterochromatin formation is gene-dose dependent, as demonstrated by the enhancement of PEV with increasing gene copies of *sov* (Fig. 5E). Furthermore, PEV analysis revealed a dominant genetic interaction between HP1a [encoded by the *Su(var)205* gene] and *sov*. Increasing the copies of the wild-type *sov* gene in $Su(var)205^5$ heterozygous flies caused decreased eye pigment production, indicating that increased amounts of Sov can compensate the heterochromatin formation defects caused by decreased HP1a levels (Fig. 5F). Haplo-suppression and triplo-enhancement of PEV by *sov*, and its genetic and physical interaction with HP1a indicates that Sov functions as a structural component of the heterochromatin.

Heterochromatin is epigenetically defined by repressive chromatin modifications, such as trimethylation of histone 3 at lysine 9 (H3K9me3), which is mediated by the histone methyl transferase *egg* and is recognized by HP1a. To test the effect of *sov* on the deposition of this repressive chromatin modification, we visualized H3K9me3 by immunostaining of sov^{del1} homozygous germline clones. In the *sov*-null mutant cells, no difference in H3K9me3 immunostaining was detectable when compared with the neighbouring *sov* heterozygous cells, indicating that Sov functions downstream of *egg* in heterochromatin formation (Fig. S7A). Similar to the wild type, HP1a was recruited to the heterochromatic foci and formed elongated structures in *sov* homozygous germline clones and in *sov* RNAi germ cells (Fig. S7B-D). To dissect further the epistatic relationship between HP1a and *sov*, we analysed Sov localization in HP1a-silenced germ cells. Wild-type Sov

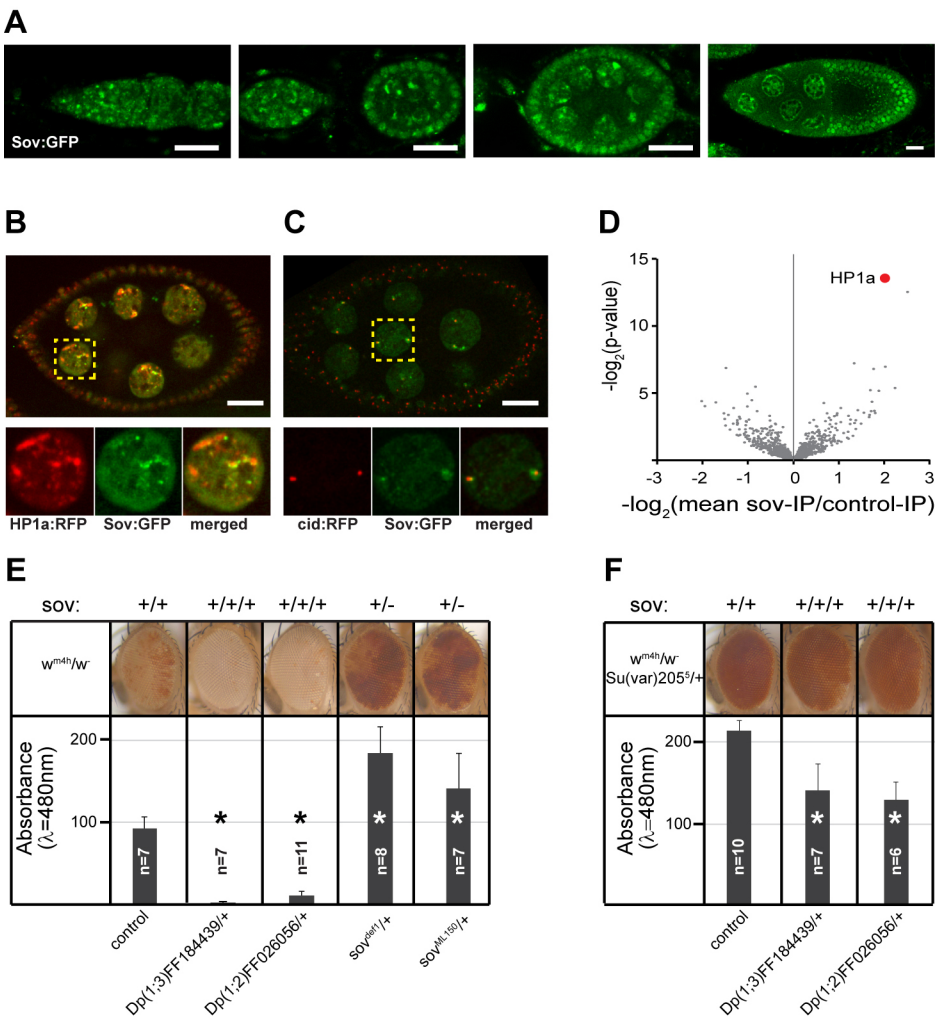

Fig. 5. Sov interacts with HP1a and promotes heterochromatin formation.
(A) Immunostaining showing localization of Sov:GFP during oogenesis. Sov localizes in the nuclei and accumulates at nuclear foci. Scale bars: 20 µm. (B,C) Living egg chambers co-expressing Sov:GFP (green) with HP1a:RFP (red) in B and with Cid:RFP (red) in C. Sov partially colocalizes with HP1a and Centrosome identifier (Cid). Scale bars: 20 µm. (D) Volcano plot showing fold enrichment values and significance levels for proteins co-immunoprecipitated with Sov:GFP from ovary lysates. HP1a (red dot) is the most significantly enriched protein. (E,F) Analysis of the modification effect of *sov* on PEV. (E,F) Adult eyes and eye pigment levels of w^{m4h}/w^{1118} (E) and w^{m4h}/w^{1118}; $Su(var)205^5$/+ (F) females carrying various numbers of wild-type copies of the *sov* gene. Data are mean±s.d.; *t*-test, $^*P<0.05$.

Development (2018) 145, dev170639. doi:10.1242/dev.170639

localization was found in HP1a RNAi cells, indicating that Sov localization does not depend on HP1a (Fig. S7E,F).

To test the involvement of Sov in HP1a-mediated gene silencing, we applied a LacI/LacO transcriptional reporter assay (Sienski et al., 2015). The NLS-GFP reporter construct containing LacO repeats was expressed in the ovary (Fig. 6A,D). We expressed LacI tagged HP1a in the germline (HP1a:LacI), which was artificially recruited to the reporter via LacI-LacO interaction. Tethering HP1a:LacI to the reporter DNA suppressed GFP expression in the germline (Fig. 6B,D). We silenced *sov* in the germline and observed no derepression of the reporter expression, suggesting that *sov* is not required for HP1a-mediated repression of the reporter locus when HP1a is artificially tethered to the DNA, but rather promotes the recruitment of HP1a to the chromatin (Fig. 6C,D).

Formation of heterochromatic domains have been shown to be driven by liquid phase separation via weak hydrophobic interaction between HP1a molecules and other heterochromatin components (Larson et al., 2017; Strom et al., 2017). In the mature heterochromatin, HP1a is mobile in the liquid compartment, whereas chromatin bound HP1a is immobile. To study the function of *sov* in the regulation of the dynamic properties of heterochromatin, we measured the immobile fraction of HP1a at the heterochromatin foci. We expressed HP1a:GFP in the germ cells and used fluorescent recovery after photobleaching (FRAP) to analyse HP1a dynamics (Movie 1). Silencing of *sov* resulted in an increase of the mobile fraction of HP1a:GFP (Fig. 6E-G). Increase of HP1a mobility indicates that *sov* stabilizes the heterochromatin domain by the enhancement of HP1a association with the chromatin polymer.

Sov promotes transcription in the heterochromatic genome regions

To determine the global effect of *sov* on steady-state mRNA levels, we compared mRNA-seq data of *nosGal4>sovRNAi* and *nosGal4>wRNAi* control ovaries. Of the 6811 euchromatic genes expressed in the ovary, transcription was increased by more than twofold at 161 genes (2.4%), whereas 146 genes had a more than twofold decrease in mRNA levels (2.1%). Of the 203 expressed genes mapping to the heterochromatic regions of the genome, 26 were downregulated more than twofold (15.1%), whereas no heterochromatic gene was upregulated (Fig. 7A). Over-representation of the heterochromatic genes in the downregulated gene set indicates that Sov preferentially promotes transcription in the heterochromatic genome regions.

Long piRNA precursors are transcribed from piRNA clusters that require a heterochromatic context for transcription (Brennecke et al., 2007; Rangan et al., 2011). We hypothesized that *sov* is involved in transposon repression by regulating piRNA cluster transcription. In the soma, piRNA clusters are uni-strand clusters, i.e. only the plus strand of the piRNA clusters is transcribed. In the germ cells, piRNA precursors are generated from both uni-strand and dual-strand clusters (Brennecke et al., 2007). We carried out strand-specific RT-qPCR for piRNA precursors derived from the germline-specific dual-strand 42AB cluster, from the germline and soma-expressed uni-strand 20A cluster, and from the soma-specific *flamenco* (*flam*) cluster. In *sov* RNAi cells, no decrease in the transcript levels was detected from the transcribed strands of cl20A cluster and *flam*; however, transcription of the dual-strand cl42AB was severely affected (Fig. 7B). Although the plus-strand-specific transcript levels were not reduced, we detected decreased piRNA precursor production from the minus strand of the cl42AB. The effect of *sov* on transcription of the minus strand of the dual-strand piRNA cluster resembles that of *egg*, suggesting that *sov* affects chromatin regulation of the cluster (Rangan et al., 2011).

To investigate the chromatin structure at the dual-strand clusters, we analysed the localization Rhino, an HP1 homologue associated exclusively with the dual-strand piRNA clusters. Silencing of *sov*

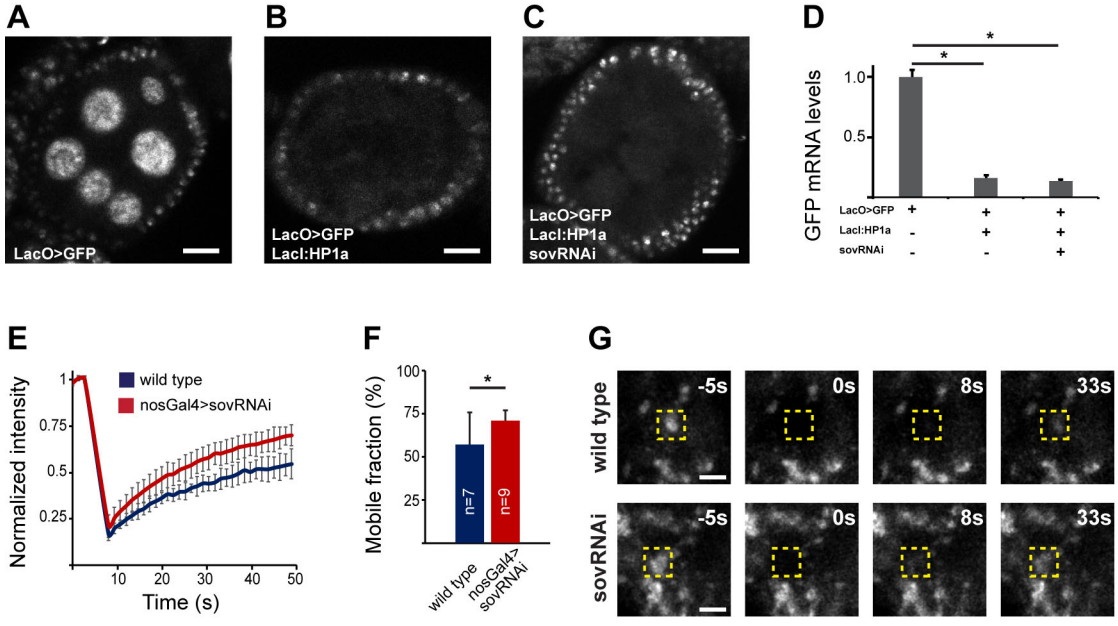

Fig. 6. Sov stabilizes heterochromatin by the enhancement of the association of HP1a with the chromatin. (A-D) A HP1a-tethering assay. (A) GFP fluorescence in egg chambers expressing the ubiquitous LacO-GFP reporter (A), the LacI:HP1a transgene (B) and the sovRNAi silencing construct (C) in the germ line. (D) Changes in GFP mRNA levels in ovaries expressing the indicated transgenes. Data are mean±s.d.; *t*-test, **P*<0.05. (E-G) Frap analysis of HP1a. Graphs showing fluorescence recovery curves (E) and mobile fractions (F) of HP1a:GFP in wild-type and *sov*-silenced germ cell nuclei. Silencing of *sov* resulted in an increased HP1a mobility. Data are mean±s.d.; *t*-test, **P*<0.05. (G) Movie frames showing recovery of HP1a:GFP fluorescence in wild-type and *nosGal4>sovRNAi* nuclei in a representative FRAP experiment. White boxes indicate photobleached regions. Scale bars: 2 µm in A-C.

Development (2018) 145, dev170639. doi:10.1242/dev.170639

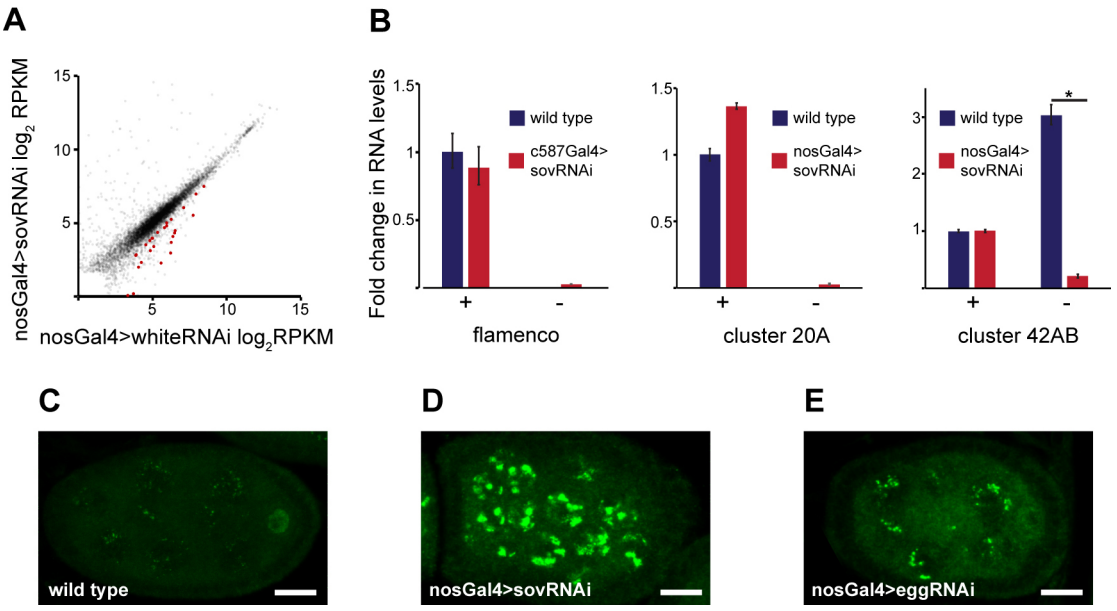

Fig. 7. Sov promotes transcription in the heterochromatic genome regions. (A) Scatter plot showing expression levels of genes (grey) in *nosGal4>sovRNAi* ovaries. Heterochromatic genes with FC>2 are in shown in red. (B) Strand-specific RT-qPCR on wild-type, *c587Gal4>sovRNAi* and *nosGal4>sovRNAi* ovaries for RNAs derived from *flamenco*, cl20A and cl42AB. Data are mean±s.d.; *t*-test, **P*<0.05. (C-E) Rhino (green) localization in wild-type (C), *sov*-silenced (D) and *egg*-silenced (E) egg chambers. Silencing of *sov* and *egg* induces formation of nuclear aggregates of Rhino. Scale bars: 20 µm.

induced formation of nuclear aggregates of Rhino, suggesting that Sov is required for the formation of the proper chromatin structure at the dual-strand piRNA clusters (Fig. 7D). Silencing of *egg* in the germline resulted in a similar abnormality in Rhino localization, supporting the hypothesis that Sov affects dual-strand cluster transcription by regulating heterochromatin structure at this cluster in cooperation with *egg* (Fig. 7E).

Next, we analysed whether *sov* silencing in the germ line affects expression of the genes involved in the piRNA pathway. Analysis of the RNA-seq data of germline-silenced *sov* ovaries revealed a significant downregulation of *Ago3*, a member of the Ago family required for piRNA biogenesis (Fig. S8A). As mature piRNAs enable Piwi to enter into the nucleus, we analysed Piwi localization in the sov^{del1} mutant and in the *sov* RNAi cells. We detected a nuclear accumulation of Piwi, indicating that the nuclear translocation of Piwi is not affected by the reduction in *Ago3* levels (Fig. S9A-F). Nevertheless, reduction of *Ago3* expression in Sov-depleted germ cells uncovers the involvement of *sov* in an additional regulatory level of the piRNA-pathway.

DISCUSSION

Sov is a novel heterochromatin component

Heterochromatin represents a functionally and structurally separate nuclear domain. The heterochromatin-associated DNA includes at least one-third of the *Drosophila* genome and is mainly composed of repetitive sequences, such as transposon fragments and satellite repeats (Hoskins et al., 2007; Smith et al., 2007). Besides its DNA content, the heterochromatin is rather epigenetically defined by a pattern of various histone modifications and by the binding of additional chromatin-associated proteins (Kharchenko et al., 2011; Riddle et al., 2011; Saha et al., 2018). Although there is a diversity of combinatorial patterns of epigenetic marks in the heterochromatin, the majority of the heterochromatin regions lack the 'activating' chromatin marks and are enriched in the 'repressive' signatures, such as H3K9me3 and HP1a (Riddle et al., 2011). In addition to the DNA and the specific protein composition, heterochromatin has a higher level of organization. HP1a is capable of demixing from solution and forming liquid droplets that organize the assembly of the heterochromatin into a membrane-less nuclear domain via liquid-liquid phase separation (Larson et al., 2017; Strom et al., 2017). Many proteins driving the formation of phase-separated organelles contain extended intrinsically disordered regions and are enriched in RGG/RG domains (Boeynaems et al., 2018; Mitrea and Kriwacki, 2016). Sov shows a remarkable structural similarity to these proteins as it has an unusually long disordered N terminus that contains an RGG/RG repeat domain. It is tempting to speculate that Sov functions, in concert with its binding partner HP1a, in the establishment of the unique physical properties of heterochromatin. Indeed, the integrity of the mature heterochromatin domain was shown to require formation of the immobile HP1a compartment through the interaction of HP1a with non-histone binding partners (Strom et al., 2017). We propose that Sov is one of these non-histone partners of HP1a. We show that Sov affects the dynamics of HP1a between the liquid and static compartments in the heterochromatin domain, suggesting that the HP1a-mediated phase separation driven heterochromatin formation depends, at least in part, on Sov. The RGG/RG domain found in Sov is a widespread RNA binding domain displaying degenerate RNA-binding specificity (Ozdilek et al., 2017). The HP1a complex containing Sov is enriched in RNAs, raising the possibility that the putative RNA binding of Sov is involved in proper heterochromatin function (Alekseyenko et al., 2014). Targeting of heterochromatin formation at particular genomic regions involves diverse mechanisms, such as function of satellite DNA-specific binding proteins or the RNAi machinery (Elgin and Reuter, 2013). In the LacI/LacO-based tethering assay, we show that HP1a-mediated repression is independent of Sov, whereas Sov enhances the recruitment and binding of HP1 to the chromatin. This function of Sov could be performed by the highly structured C terminus, which contains a large number of tandem Zn fingers. Through these domains, Sov may stabilize the binding of HP1a complexes to specific DNA sequences and target Sov/HP1a-mediated processes at specific regions of the genome.

Development (2018) 145, dev170639. doi:10.1242/dev.170639

Heterochromatin is usually associated with transcriptional repression. Many protein-coding genes residing in the repressive domains, however, require the heterochromatic environment for transcription (Clegg et al., 1998; Lu et al., 2000; Schulze et al., 2005; Wakimoto and Hearn, 1990). Disruption of heterochromatin by impaired HP1a function results in reduced expression of these genes (Lundberg et al., 2013). Consistent with this observation, Sov preferentially promotes the transcription of heterochromatin-resident genes by positively regulating HP1a function.

Sov is involved in transposon repression

We demonstrate that Sov is involved in the regulation of transposon repression at multiple levels. In the germline, it is required for proper transcription of the piRNA clusters and promotes the expression of the piRNA-pathway component Ago3. In addition, it may mediate transcriptional gene silencing, both in the germline and in the somatic cells.

Efficient transcription of the piRNA clusters requires a heterochromatic environment. Despite the obvious differences in their regulation, both uni-strand and dual-strand clusters were shown to be enriched in the repressive H3k9me3 histone mark (Mohn et al., 2014). Impairment of heterochromatin formation leads to reduction of piRNA cluster transcription (Rangan et al., 2011; Teo et al., 2018). The transcription of the uni-strand clusters critically depends on *egg*, however; in particular, the minus strand of the dual-stranded cl42AB was sensitive to *egg* depletion (Rangan et al., 2011). Similar to *egg*, depletion of *sov* results in reduction of the transcription of the minus strand of the cl42AB, whereas the transcription of the plus strand remains unaffected. The effect of *egg* and *sov* depletion on cluster transcription, however, is not identical. In contrast to *egg*, the function of *sov* is restricted to the dual-stranded cluster (Rangan et al., 2011). It is possible that *sov* specifically regulates the formation of the Rhino-dependent specialized heterochromatin that enables dual-stranded transcription. Further studies are needed to explore how this separation in *sov* function is regulated.

Another level of transposon regulation, where Sov is involved, is the indirect control of piRNA biogenesis. Like *egg*, *sov* is required for *Ago3* transcription, raising the possibility that the transposon derepression defects found in *sov*-depleted germ cells may result not only from reduced cluster transcription, but also from defective piRNA biogenesis (Kang et al., 2018). However, the effect of *sov* on transposon repression and niche regulation differs from that of *Ago3*. Unlike *egg* or *sov* mutants, no GSC loss was detected in the *Ago3* mutants, showing that GSC self-renewal was not affected (Rojas-Ríos et al., 2017). Consistent with the lack of GSC self-renewal defect in *Ago3* mutants, piRNAs are produced in the absence of Ago3 through an Aub-dependent homotypic amplification mechanism, and these piRNAs could be used in the regulation of GSCs (Wang et al., 2015a). piRNAs enable Piwi to move from the cytoplasm to the nucleus, where it suppresses transposon transcription (Klenov et al., 2011; Le Thomas et al., 2013; Rozhkov et al., 2013; Sienski et al., 2015; Wang and Elgin, 2011; Yashiro et al., 2018). In *sov* mutant and *sov* RNAi cells, we detect nuclear Piwi accumulation, suggesting that piRNA biogenesis was not completely abolished. Loss of Ago3 results in the derepression of a subset of transposons (Wang et al., 2015a). Sov depletion, however, causes a stronger defect in transposon regulation, i.e. the derepression of all transposon classes, indicating that *sov* has a more general effect on transposon silencing than the sole enhancement of *Ago3* transcription.

In the *sov* RNAi ECs, we find a derepression of the *gypsy* transposon. piRNAs required for *gypsy* silencing are generated from the *flam* cluster. Similar to HP1a, Sov is dispensable for *flam* transcription (Penke et al., 2016). As there is no Ago3-dependent piRNA amplification in the soma, Sov must have an additional effect on transposon silencing. An attractive explanation for *gypsy* derepression in the Sov-depleted ECs could be that *sov* is involved in the transcriptional transposon silencing mechanism. This step of the silencing pathway requires heterochromatinization of the transposon locus. Tethering of the Piwi-RISC to the transposon induces the recruitment of the effector complex, composed of Asterix, Panx, Mael and Egg, to the transposon loci (Sienski et al., 2012, 2015; Yu et al., 2015). Egg initiates the deposition of the repressive H3K9me3 mark and inhibits transcription by recruiting HP1a. In a parallel pathway, Piwi also recruits Histone1 to the transposons, which organizes the chromatin into a higher order repressive state (Iwasaki et al., 2016). Sov physically interacts with HP1a and stabilizes the heterochromatin domain through the enhancement of an association of HP1a with the chromatin. We propose that Sov supports the recruitment of HP1a to the transposon locus by binding to HP1a, which in turn stabilizes the association of H3K9me3-bound HP1a with the chromatin. A similar Sov-mediated mechanism might work also in the germline; however, this requires further investigation.

Sov functions in the stem cell niche

We show that Sov is involved in germ cell development by regulating GSC survival, GSC differentiation and EC survival. The complex loss-of-function phenotype of *sov* closely resembles that of *egg* mutations, supporting our hypothesis that *sov* contributes to the formation and maintenance of the HP1a-Egg-mediated repressive chromatin environment (Wang et al., 2011).

Germline-specific RNAi revealed that Sov is required in the GSCs to control their self-renewal in a cell-autonomous manner. Loss of function of the components of the heterochromatin machinery and of the piRNA pathway induce apoptotic GSC loss accompanied with transposon derepression, DNA damage and checkpoint activation (Chen et al., 2007; Klattenhoff et al., 2007; Ma et al., 2014, 2017). In *egg* mutants, upregulation of the apoptotic genes *hid* and *reaper*, and activation of Caspase 3 cleavage was found (Clough et al., 2007; Kang et al., 2018). Similarly, we observed an accumulation of DNA damage, checkpoint activation and apoptosis in *sov*-depleted cells. We propose that *sov* ensures GSC maintenance through suppression of transposon activity-induced genome damage and, by so doing, supresses the apoptosis of the germ cells.

Cell-type specific RNAi experiments showed that Sov function is required in ECs for controlling both the maintenance and the differentiation of germ cells in a non-cell-autonomous manner. When anterior-most ECs are lost, GSCs are gradually eliminated from the niche, whereas loss of posterior ECs leads to differentiation defects and to the formation of GSC tumours (Wang and Page-McCaw, 2018). Indeed, somatic *sov* RNAi resulted in loss of both the anterior and the posterior ECs and, as a consequence, a combination of the GSC loss and germ cell tumour phenotypes was observed.

The *sov*-dependent EC loss may be induced by the improper function of the signalling network operating in the somatic niche. We show that *sov* has an effect on the *Wnt* and *dpp* signalling pathways. *Wnt* signalling was shown to promote survival of ECs and inhibit the expansion of *dpp* activity in the niche (Wang et al., 2011, 2015b). Interestingly, transposon derepression results in decreased Wnt4 expression (Upadhyay et al., 2016). We show that *sov* is required for Wnt4 expression in the ECs; however, the differentiation defect

Development (2018) 145, dev170639. doi:10.1242/dev.170639

induced by *sov* depletion is not rescued by simultaneous Wnt overexpression, indicating additional diverse roles of *sov* in ensuring EC survival.

In ECs, increasing transposon activity by knocking down *egg*, *hp1a*, *piwi* or *flam* results in cell death (Ma et al., 2014; Upadhyay et al., 2016; Wang et al., 2011). Because in *sov*-depleted ECs, we detected robust transposon derepression accompanied by caspase activation, we propose that Sov supresses EC death by downregulating transposons.

MATERIALS AND METHODS

Drosophila stocks

All animals were raised at 25°C, unless otherwise indicated. The sov^{del1} allele was generated by FRT-mediated recombination between PBac{WH}f04480 and P{XP}d07849 transposon insertions (Ryder et al., 2004). The sov^{2} and sov^{ML150} alleles were obtained from the Bloomington Drosophila Stock Center. To silence *sov*, we generated the *UAS-sovRNAi[3-2]* transgenic construct expressing shRNA targeting the last exon of *sov*. In this study, the *UAS-sovRNAi[3-2]* construct was used for *sov* silencing unless otherwise indicated. The Dp(1;3)FF184439 and Dp(1;2)FF026056 duplications were generated by inserting the FF184439 and the FF026056 fosmid constructs into the attP2 and attP40 docking sites, respectively (Ejsmont et al., 2011). The FlyFos018439-CG14438-SGFP-V5-preTEV-BLRP-3XFLAG fosmid was obtained from the Drosophila TransgeneOme Project and was inserted into the attP40 site. For the sake of simplicity, we refer to this transgenic line as Sov:GFP thereafter.

The strains used in this study include: sov^{2} (Bl#4611), sov^{ML150} (Bl#4591), *bam-GFP* (Chen and McKearin, 2003), *nos-Gal4* (Van Doren et al., 1998), *c587Gal4* (Manseau et al., 1997; Song et al., 2004), *hs-bam* (Ohlstein and McKearin, 1997), *gypsy-LacZ* (Dönertas et al., 2013), *Burdock-LacZ* (Dönertas et al., 2013), *Het-A-LacZ* (Dönertas et al., 2013), *Vasa:AID:GFP* (Bl# 76126) (Bence et al., 2017), *HP1a:RFP* (BL#30562) (Wen et al., 2008), *HP1a:GFP* (BL#30561) (Wen et al., 2008), *FRT19A,His2Av:GFP,hsFLP/FRT19A; His2Av-mRFP* (B#30563), FRT19A (Bl#1709), $Su(var)205^{5}$ (Bl#6234), w^{m4h}, *UAS-HP1aRNAi-TRiP.GL00531* (Bl#36792), *UAS-eggRNAi-TRiP.HMS00443* (Bl#32445), *UAS-wRNAi-TRiP.HMS0001* (Bl#33623), *UAS-sovRNAi-TRiP.HMC04875* (Bl#57558), *UAS-sovRNAi-KK103679* (VDRC#v100109), *8XLacO-nos>GFP* (Sienski et al., 2015), *UASP-LacI:HP1a* (Sienski et al., 2015), *UAS-Wnt4.ORF.3XHA* (FlyORF#F001112), *UAS-dWnt4(r13)* (Sato et al., 2006) and *oskMS2/MS2GFP* (Forrest and Gavis, 2003; Zimyanin et al., 2008).

Sequencing of the sov^{2} mutant allele

To sequence the sov^{2} mutant allele, genomic DNA was isolated from sov^{2}/sov^{del1} mutant females and the *sov*-coding sequence, including the introns, was PCR amplified and sequenced between the start and the stop codons. Comparison of the sov^{2} sequence with the reference R6.15 *Drosophila* genomic sequence revealed 20 missense mutations, a 27 bp in-frame deletion, a 54 bp in-frame insertion and a frame-shift mutation in the sov^{2}-coding region. To unambiguously identify the mutation responsible for the *sov* mutant phenotype, we sequenced the *sov*-coding sequence of the $wisp^{12\text{-}3147}$ allele and used it as a reference. The $wisp^{12\text{-}3147}$ and the sov^{2} alleles were isolated in the same genetic screen and have the same paternal chromosome (Mohler, 1977). Analysis of the sequences revealed that all mutations are shared between sov^{2} and $wisp^{12\text{-}3147}$, except for the frame-shift mutation.

Clone induction and cell type-specific silencing

The negatively marked control and *sov* mutant EC and germline clones were generated using the FLP/FRT-mediated recombination as described previously (Song et al., 2002; Xie and Spradling, 1998). Briefly, heterozygous *sov* mutant and wild-type control cells ubiquitously express both Histone2Av:RFP and Histone2Av:GFP. Upon mitotic recombination, cells become homozygous for the *sov* mutant allele and concomitantly lose Histone2Av:GFP expression. Thus, homozygous *sov* mutant clones express only Histone2Av:RFP and can be identified by their lack of Histone2Av:GFP expression. To generate *sov* mutant clones, *FRT19A,His2Av:GFP, hsFLP/FRT19A,*sov^{del1}*; His2Av-mRFP/+* females were heat shocked either 24 h after egg laying or at the adult stage. Young females were heat shocked on three consecutive days for 1 h at 37°C, and the mutant phenotypes were examined 6 days after clone induction.

To silence *sov* in the germ line, the *nos-Gal4* driver was used. To silence *sov* in the ECs specifically at the adult stage, *c587Gal4/UAS-sovRNAi[3-2]; TubGal80*^{ts} females were cultured at 18°C until adulthood and then shifted to 29°C. For the transposon sensor assay, *sov* was silenced using the germ line-specific MTDGal4 driver. To express Bam in *sov* mutants, sov^{2}/sov^{ML150}*; hs-bam* flies were heat-shocked at 37°C twice for 1 h, separated by a 2-h recovery period at 25°C. Ovaries were analysed 24 h after the first heat-shock.

Position effect variegation assay

Female flies were aged at 25°C for 10 days prior to imaging. To measure eye pigmentation, females were frozen in liquid nitrogen. Heads were separated from bodies by brief vortexing. Samples of 10 females were homogenized in 0.5 ml of 0.01 M HCl in ethanol; the homogenate was placed at 4°C overnight, warmed at 50°C for 5 min, clarified by centrifugation and the OD at 480 nm of the supernatant was measured.

Immunohistochemistry and FRAP

β-Gal staining of transposon sensor lines was performed as described previously (Dönertas et al., 2013). Immunostainings were performed as described earlier (Jankovics et al., 2014). The list of primary antibodies used is summarized in Table S1. DAPI was used to label the nuclei, actin was visualized by phalloidin staining. Specimens were examined with Leica TCS SP5 confocal microscope. To determine the number of escort cells, niches were co-immunostained with Traffic jam (Tj) and Fas3 antibodies. Terminal filament cells were double-negative, follicle cells were labelled by both antibodies, whereas ECs and cap cells were labelled exclusively by Tj. Then, cap cells and escort cells were distinguished based on their location, shapes of nuclei and based on the weaker intensity of Tj labelling in the cap cells (Wang and Page-McCaw, 2018).

For live imaging of Sov:GFP, HP1a:GFP, HP1a:RFP and Cid:RFP, samples were prepared as described previously (Forrest and Gavis, 2003) and examined with a VisiScope spinning disc confocal microscope. Fluorescence recovery experiments were performed on stage 10 egg chambers expressing HP1a:GFP. FRAP experiments were performed with a Leica SP5 confocal microscope. The 405 nm laser line was used to photobleach a 4 μm^2 region of the heterochromatin domain. Recovery was recorded for 1 min at one frame every 1.5 s. Fluorescence recovery curves were analysed using the easyFrap software as described previously (Bancaud et al., 2010; Koulouras et al., 2018). Statistical tests were performed with GraphPad Prism.

Co-immunoprecipitation and mass spectrometry

For the protein interactome analysis, 2-day-old *Sov:GFP* and w^{1118} females were used. Ovaries were dissected in PBS. Ovaries (150-200 µl) were harvested, frozen in liquid nitrogen and ground with TissueLyser at 30 Hz. Total proteins from *Drosophila* tissue were extracted using the manufacturer's Lysis buffer supplemented with 1 mM DTT, 1 mM PMSF, 1×Sigma protease inhibitor cocktail, 3 mM pNPP and 1 µM MG132. Total protein extracts (8 mg/immunoprecipitate) were immunopurified using anti-GFP (three replicates) or anti-FLAG (three replicates) antibody coupled 50 nm magnetic beads (MACS Technology, Miltenyi) digested in column with trypsin, and analysed in a single run using a mass spectrometer (Hubner et al., 2010)

The resulting peptide mixture was desalted prior to LC-MS/MS analysis (Omix C18 100 µl tips, Varian) and the purified peptide mixture was analysed by LC-MS/MS using a nanoflow RP-HPLC on-line coupled to a linear ion trap-Orbitrap (Orbitrap-Elite, ThermoFisher Scientific) mass spectrometer operating in positive ion mode. Data acquisition was carried out in data-dependent fashion, the 10 most abundant, multiply charged ions were selected from each MS survey for MS/MS analysis (MS spectra were acquired in the Orbitrap; CID spectra were acquired in the linear ion trap).

Raw data were converted into peak lists using the in-house PAVA software (Guan et al., 2011) and searched against the Swissprot database using the Protein Prospector search engine (v5.15.1) with the following parameters: enzyme, trypsin with maximum 1 missed cleavage; mass accuracies, 5 ppm for precursor ions and 0.6 Da for fragment ions (both monoisotopic); fixed

Development (2018) 145, dev170639. doi:10.1242/dev.170639

modification, carbamidomethylation of Cys residues; variable modifications, acetylation of protein N-termini; Met oxidation, cyclization of N-terminal Gln residues allowing a maximum of two variable modifications per peptide. Acceptance criteria were: minimum scores, 22 and 15; maximum E values, 0.01 and 0.05 for protein and peptide identifications, respectively. Another database search was also performed using the same search and acceptance parameters except that the Uniprot.random.concat database (downloaded 2015/4/16) was searched with *Drosophila melanogaster* species restriction (52,524 proteins), including additional proteins identified from the previous Swissprot search (protein score>50). False discovery rate was estimated using peptide identifications representing randomized proteins (2×number of random IDs/total peptide IDs)=2× number of random IDs divided by peptide IDs.

Spectral counting was used to estimate relative abundance of individual proteins in the Sov:GFP and control samples: peptide counts of the individual proteins were normalized to the total number of peptide identifications in each sample, then these normalized peptide counts were compared in the two samples. Enrichment between SovGFP and control experiments was calculated using edgeR (Li and Andrade, 2017). Counts representing Sov were omitted from the analysis.

RT-quantitative PCR

In general, the total RNA was prepared from whole ovaries using ReliaPrep RNA Tissue Miniprep System (Promega, Z6111). cDNAs were synthesized using oligodT primers (First Strand cDNA Synthesis kit, ThermoScientific, K1612). Strand-specific RT-qPCR was performed as described previously (Klattenhoff et al., 2009). For strand-specific RT-qPCR of the 42AB and 20A piRNA clusters, ovaries of 2-day-old *nosGal4>sovRNAi* females were used. For strand-specific RT-qPCR of the *flam* cluster, *c587Gal4>sovRNAi; Tub>Gal80^{ts}* females were cultured on 18°C and shifted to 29°C at the adult stage. RT-qPCR was performed 10 days after the temperature shift. qPCR reactions were performed using Maxima SYBR Green/ROX (ThermoScientific, K0221). For each reaction, tree technical replicates were performed on three biological replicates. Rp49 transcript was used as internal control. Data ware analysed using the Rotor-Gene Q Series software. Primer sequences are provided in Table S2.

RNA-sequencing and data analysis

For RNA-seq, ovaries of *nosGal4>sovRNAi3-2* and *nosGal4>wRNAi* females were dissected. Total RNA was prepared using RNeasy Mini Kit (Qiagen, 74104). RNA samples were quantified and their quality determined by capillary gel electrophoresis with a 2100 Bioanalyzer (Agilent) instrument using Agilent RNA 6000 nano kit. Poly(A) RNAs were selected using the NEBNext Poly(A) mRNA Magnetic Isolation Module then strand-specific RNA-seq libraries were prepared using the NEBNext Ultra RNA Library Prep Kit for Illumina with NEBNext Multiplex Oligos for Illumina following the recommendations of the manufacturer (New England Biolabs). Sequencing libraries were validated and quantified using an Agilent DNA 1000 kit in a 2100 Bioanalyzer instrument. After pooling, paired-end sequencing was carried out with an Illumina MiSeq instrument using MiSeq Reagent kit V3-150.

Fastq files were generated with MiSeq Control Software then quality trimmed and filtered with Trimmomatic v0.33. For transcriptome analysis sequence flies were aligned to the *Drosophila melanogaster* reference genome r6.13 with Tophat v2.0.9. After alignment files were deduplicated with SAMtools software and differential expression analysis was performed with CuffDiff v2.1.1 using the corresponding transcript annotation file. For transposon expression, analysis-trimmed fastq files were aligned to the USCS dm6 reference genome with Bowtie v2.1 then differential transposon expression was determined by CuffDiff v2.1.1 using a corresponding transposon annotation file (labshare.cshl.edu/shares/mhammelllab/www-data/TEToolkit/TE_GTF/) (Jin et al., 2015). All raw sequence data have been deposited in the SRA (www.ncbi.nlm.nih.gov/sra) under accession number PRJNA495606.

Acknowledgements

We thank W. Theurkauf, T. Tetsuya, D. McKearin, L. Gilboa and J. Brennecke for fly stocks and reagents. We also thank B. Irvine for critical reading of the manuscript.

Competing interests

The authors declare no competing or financial interests.

Author contributions

Conceptualization: F.J., M.B., M.E.; Methodology: F.J., M.B.; Software: F.J., L.B., A.P.-S., K.I.; Validation: F.J., R.S., A.P., K.I.; Formal analysis: F.J., M.B., R.S., A.F., L.B., A.P.-S., K.I., M.E.; Investigation: F.J., M.B., R.S., A.F., L.B., A.P.-S., K.I., Z.T., A.B.S.-K., M.E.; Resources: F.J., M.B., A.P.-S.; Data curation: F.J., M.B., L.B., A.P.-S., M.E.; Writing - original draft: F.J., L.B., A.P.-S., M.E.; Writing - review & editing: F.J., M.E.; Visualization: F.J.; Supervision: F.J., M.E.; Project administration: F.J., M.E.; Funding acquisition: F.J., M.E.

Funding

This work was supported by grants from the Nemzeti Kutatási, Fejlesztési és Innovációs Hivatal and the Országos Tudományos Kutatási Alapprogramok (NKFIH-K112294, NKFIH-K117010, OTKA-K108538, NKFIH-PD124446, GINOP-2.3.2-15-2016-00032 and GINOP-2.3.2.-15-2016-00001). M.B. is supported by a János Bolyai Fellowship.

Data availability

All raw sequence data have been deposited in the SRA (www.ncbi.nlm.nih.gov/sra) under accession number PRJNA495606.

Supplementary information

Supplementary information available online at
http://dev.biologists.org/lookup/doi/10.1242/dev.170639.supplemental

References

Abdu, U., Brodsky, M. and Schüpbach, T. (2002). Activation of a meiotic checkpoint during Drosophila oogenesis regulates the translation of Gurken through Chk2/Mnk. *Curr. Biol.* **12**, 1645-1651.

Alekseyenko, A. A., Gorchakov, A. A., Zee, B. M., Fuchs, S. M., Kharchenko, P. V. and Kuroda, M. I. (2014). Heterochromatin-associated interactions of Drosophila HP1a with dADD1, HIPP1, and repetitive RNAs. *Genes Dev.* **28**, 1445-1460.

Bancaud, A., Huet, S., Rabut, G. and Ellenberg, J. (2010). Fluorescence perturbation techniques to study mobility and molecular dynamics of proteins in live cells: FRAP, photoactivation, photoconversion, and FLIP. *Cold Spring Harb. Protoc.* **2010**, pdb.top90.

Bannister, A. J., Zegerman, P., Partridge, J. F., Miska, E. A., Thomas, J. O., Allshire, R. C. and Kouzarides, T. (2001). Selective recognition of methylated lysine 9 on histone H3 by the HP1 chromo domain. *Nature* **410**, 120-124.

Bence, M., Jankovics, F., Lukácsovich, T. and Erdélyi, M. (2017). Combining the auxin-inducible degradation system with CRISPR/Cas9-based genome editing for the conditional depletion of endogenous Drosophila melanogaster proteins. *FEBS J.* **284**, 1056-1069.

Boeynaems, S., Alberti, S., Fawzi, N. L., Mittag, T., Polymenidou, M., Rousseau, F., Schymkowitz, J., Shorter, J., Wolozin, B., Van Den Bosch, L. et al. (2018). Protein phase separation: a new phase in cell biology. *Trends Cell Biol.* **28**, 420-435.

Brennecke, J., Aravin, A. A., Stark, A., Dus, M., Kellis, M., Sachidanandam, R. and Hannon, G. J. (2007). Discrete small RNA-generating loci as master regulators of transposon activity in Drosophila. *Cell* **128**, 1089-1103.

Brutlag, D., Carlson, M., Fry, K. and Hsieh, T. S. (1978). DNA sequence organization in Drosophila heterochromatin. *Cold Spring Harb. Symp. Quant. Biol.* **42**, 1137-1146.

Bryan, L. C., Weilandt, D. R., Bachmann, A. L., Kilic, S., Lechner, C. C., Odermatt, P. D., Fantner, G. E., Georgeon, S., Hantschel, O., Hatzimanikatis, V. et al. (2017). Single-molecule kinetic analysis of HP1-chromatin binding reveals a dynamic network of histone modification and DNA interactions. *Nucleic Acids Res.* **45**, 10504-10517.

Chen, D. and McKearin, D. M. (2003). A discrete transcriptional silencer in the bam gene determines asymmetric division of the Drosophila germline stem cell. *Development* **130**, 1159-1170.

Chen, Y., Pane, A. and Schüpbach, T. (2007). Cutoff and aubergine mutations result in retrotransposon upregulation and checkpoint activation in Drosophila. *Curr. Biol.* **17**, 637-642.

Chen, S., Wang, S. and Xie, T. (2011). Restricting self-renewal signals within the stem cell niche: multiple levels of control. *Curr. Opin. Genet. Dev.* **21**, 684-689.

Clegg, N. J., Honda, B. M., Whitehead, I. P., Grigliatti, T. A., Wakimoto, B., Brock, H. W., Lloyd, V. K. and Sinclair, D. A. R. (1998). Suppressors of position-effect variegation in Drosophila melanogaster affect expression of the heterochromatic gene light in the absence of a chromosome rearrangement. *Genome* **41**, 495-503.

Clough, E., Moon, W., Wang, S., Smith, K. and Hazelrigg, T. (2007). Histone methylation is required for oogenesis in Drosophila. *Development* **134**, 157-165.

Czech, B., Preall, J. B., McGinn, J. and Hannon, G. J. (2013). A transcriptome-wide RNAi screen in the Drosophila ovary reveals factors of the germline piRNA pathway. *Mol. Cell* **50**, 749-761.
Dönertas, D., Sienski, G. and Brennecke, J. (2013). Drosophila Gtsf1 is an essential component of the Piwi-mediated transcriptional silencing complex. *Genes Dev.* **27**, 1693-1705.
Ejsmont, R. K., Bogdanzaliewa, M., Lipinski, K. A. and Tomancak, P. (2011). Production of fosmid genomic libraries optimized for liquid culture recombineering and cross-species transgenesis. *Methods Mol. Biol.* **772**, 423-443.
Elgin, S. C. R. and Reuter, G. (2013). Position-effect variegation, heterochromatin formation, and gene silencing in Drosophila. *Cold Spring Harb. Perspect. Biol.* **5**, a017780.
Eliazer, S. and Buszczak, M. (2011). Finding a niche: studies from the Drosophila ovary. *Stem Cell Res. Ther.* **2**, 45.
Forrest, K. M. and Gavis, E. R. (2003). Live imaging of endogenous RNA reveals a diffusion and entrapment mechanism for nanos mRNA localization in Drosophila. *Curr. Biol.* **13**, 1159-1168.
Ghabrial, A. and Schüpbach, T. (1999). Activation of a meiotic checkpoint regulates translation of Gurken during Drosophila oogenesis. *Nat. Cell Biol.* **1**, 354-357.
Guan, S., Price, J. C., Prusiner, S. B., Ghaemmaghami, S. and Burlingame, A. L. (2011). A data processing pipeline for mammalian proteome dynamics studies using stable isotope metabolic labeling. *Mol. Cell. Proteomics* **10**, M111.010728.
Heitz, E. (1928). Das Heterochromatin der Moose. *Jahrb. Für Wiss. Bot.* **69**, 762-818.
Hoskins, R. A., Carlson, J. W., Kennedy, C., Acevedo, D., Evans-Holm, M., Frise, E., Wan, K. H., Park, S., Mendez-Lago, M., Rossi, F. et al. (2007). Sequence finishing and mapping of Drosophila melanogaster heterochromatin. *Science* **316**, 1625-1628.
Huang, X., Fejes Tóth, K. and Aravin, A. A. (2017). piRNA Biogenesis in Drosophila melanogaster. *Trends Genet.* **33**, 882-894.
Hubner, N. C., Bird, A. W., Cox, J., Splettstoesser, B., Bandilla, P., Poser, I., Hyman, A. and Mann, M. (2010). Quantitative proteomics combined with BAC TransgeneOmics reveals in vivo protein interactions. *J. Cell Biol.* **189**, 739-754.
Iwasaki, Y. W., Murano, K., Ishizu, H., Shibuya, A., Iyoda, Y., Siomi, M. C., Siomi, H. and Saito, K. (2016). Piwi modulates chromatin accessibility by regulating multiple factors including histone H1 to repress transposons. *Mol. Cell* **63**, 408-419.
Jankovics, F., Henn, L., Bujna, Á., Vilmos, P., Spirohn, K., Boutros, M. and Erdélyi, M. (2014). Functional analysis of the Drosophila embryonic germ cell transcriptome by RNA interference. *PLoS ONE* **9**, e98579.
Jin, Z., Flynt, A. S. and Lai, E. C. (2013). Drosophila piwi mutants exhibit germline stem cell tumors that are sustained by elevated Dpp signaling. *Curr. Biol.* **23**, 1442-1448.
Jin, Y., Tam, O. H., Paniagua, E. and Hammell, M. (2015). TEtranscripts: a package for including transposable elements in differential expression analysis of RNA-seq datasets. *Bioinformatics* **31**, 3593-3599.
Kang, I., Choi, Y., Jung, S., Lim, J. Y., Lee, D., Gupta, S., Moon, W. and Shin, C. (2018). Identification of target genes regulated by the Drosophila histone methyltransferase Eggless reveals a role of Decapentaplegic in apoptotic signaling. *Sci. Rep.* **8**, 7123.
Kharchenko, P. V., Alekseyenko, A. A., Schwartz, Y. B., Minoda, A., Riddle, N. C., Ernst, J., Sabo, P. J., Larschan, E., Gorchakov, A. A., Gu, T. et al. (2011). Comprehensive analysis of the chromatin landscape in Drosophila melanogaster. *Nature* **471**, 480-485.
Klattenhoff, C., Bratu, D. P., McGinnis-Schultz, N., Koppetsch, B. S., Cook, H. A. and Theurkauf, W. E. (2007). Drosophila rasiRNA pathway mutations disrupt embryonic axis specification through activation of an ATR/Chk2 DNA damage response. *Dev. Cell* **12**, 45-55.
Klattenhoff, C., Xi, H., Li, C., Lee, S., Xu, J., Khurana, J. S., Zhang, F., Schultz, N., Koppetsch, B. S., Nowosielska, A. et al. (2009). The Drosophila HP1 homolog Rhino is required for transposon silencing and piRNA production by dual-strand clusters. *Cell* **138**, 1137-1149.
Klenov, M. S., Sokolova, O. A., Yakushev, E. Y., Stolyarenko, A. D., Mikhaleva, E. A., Lavrov, S. A. and Gvozdev, V. A. (2011). Separation of stem cell maintenance and transposon silencing functions of Piwi protein. *Proc. Natl. Acad. Sci. USA* **108**, 18760-18765.
Koulouras, G., Panagopoulos, A., Rapsomaniki, M. A., Giakoumakis, N. N., Taraviras, S. and Lygerou, Z. (2018). EasyFRAP-web: a web-based tool for the analysis of fluorescence recovery after photobleaching data. *Nucleic Acids Res.* **46**, W467-W472.
Larson, A. G., Elnatan, D., Keenen, M. M., Trnka, M. J., Johnston, J. B., Burlingame, A. L., Agard, D. A., Redding, S. and Narlikar, G. J. (2017). Liquid droplet formation by HP1α suggests a role for phase separation in heterochromatin. *Nature* **547**, 236-240.
Le Thomas, A., Rogers, A. K., Webster, A., Marinov, G. K., Liao, S. E., Perkins, E. M., Hur, J. K., Aravin, A. A. and Tóth, K. F. (2013). Piwi induces piRNA-guided transcriptional silencing and establishment of a repressive chromatin state. *Genes Dev.* **27**, 390-399.
Li, Y. and Andrade, J. (2017). DEApp: an interactive web interface for differential expression analysis of next generation sequence data. *Source Code Biol. Med.* **12**, 2.
Li, M. A., Alls, J. D., Avancini, R. M., Koo, K. and Godt, D. (2003). The large Maf factor Traffic Jam controls gonad morphogenesis in Drosophila. *Nat. Cell Biol.* **5**, 994-1000.
Lin, H. and Spradling, A. C. (1993). Germline stem cell division and egg chamber development in transplanted Drosophila germaria. *Dev. Biol.* **159**, 140-152.
Lu, B. Y., Emtage, P. C., Duyf, B. J., Hilliker, A. J. and Eissenberg, J. C. (2000). Heterochromatin protein 1 is required for the normal expression of two heterochromatin genes in Drosophila. *Genetics* **155**, 699-708.
Lundberg, L. E., Stenberg, P. and Larsson, J. (2013). HP1a, Su(var)3-9, SETDB1 and POF stimulate or repress gene expression depending on genomic position, gene length and expression pattern in Drosophila melanogaster. *Nucleic Acids Res.* **41**, 4481-4494.
Ma, X., Wang, S., Do, T., Song, X., Inaba, M., Nishimoto, Y., Liu, L., Gao, Y., Mao, Y., Li, H. et al. (2014). Piwi is required in multiple cell types to control germline stem cell lineage development in the Drosophila ovary. *PLoS ONE* **9**, e90267.
Ma, X., Zhu, X., Han, Y., Story, B., Do, T., Song, X., Wang, S., Zhang, Y., Blanchette, M., Gogol, M. et al. (2017). Aubergine controls germline stem cell self-renewal and progeny differentiation via distinct mechanisms. *Dev. Cell* **41**, 157-169.e5.
Malone, C. D., Brennecke, J., Dus, M., Stark, A., McCombie, W. R., Sachidanandam, R. and Hannon, G. J. (2009). Specialized piRNA pathways act in germline and somatic tissues of the Drosophila ovary. *Cell* **137**, 522-535.
Manseau, L., Baradaran, A., Brower, D., Budhu, A., Elefant, F., Phan, H., Philp, A. V., Yang, M., Glover, D., Kaiser, K. et al. (1997). GAL4 enhancer traps expressed in the embryo, larval brain, imaginal discs, and ovary of Drosophila. *Dev. Dyn.* **209**, 310-322.
McKearin, D. and Ohlstein, B. (1995). A role for the Drosophila bag-of-marbles protein in the differentiation of cystoblasts from germline stem cells. *Development* **121**, 2937-2947.
Mitrea, D. M. and Kriwacki, R. W. (2016). Phase separation in biology; functional organization of a higher order. *Cell Commun. Signal.* **14**, 1.
Mohler, J. D. (1977). Developmental genetics of the Drosophila egg. I. Identification of 59 sex-linked cistrons with maternal effects on embryonic development. *Genetics* **85**, 259-272.
Mohn, F., Sienski, G., Handler, D. and Brennecke, J. (2014). The rhino-deadlock-cutoff complex licenses noncanonical transcription of dual-strand piRNA clusters in Drosophila. *Cell* **157**, 1364-1379.
Mottier-Pavie, V. I., Palacios, V., Eliazer, S., Scoggin, S. and Buszczak, M. (2016). The Wnt pathway limits BMP signaling outside of the germline stem cell niche in Drosophila ovaries. *Dev. Biol.* **417**, 50-62.
Muerdter, F., Guzzardo, P. M., Gillis, J., Luo, Y., Yu, Y., Chen, C., Fekete, R. and Hannon, G. J. (2013). A genome-wide RNAi screen draws a genetic framework for transposon control and primary piRNA biogenesis in Drosophila. *Mol. Cell* **50**, 736-748.
Ohlstein, B. and McKearin, D. (1997). Ectopic expression of the Drosophila Bam protein eliminates oogenic germline stem cells. *Development* **124**, 3651-3662.
Ozdilek, B. A., Thompson, V. F., Ahmed, N. S., White, C. I., Batey, R. T. and Schwartz, J. C. (2017). Intrinsically disordered RGG/RG domains mediate degenerate specificity in RNA binding. *Nucleic Acids Res.* **45**, 7984-7996.
Peacock, W. J., Lohe, A. R., Gerlach, W. L., Dunsmuir, P., Dennis, E. S. and Appels, R. (1978). Fine structure and evolution of DNA in heterochromatin. *Cold Spring Harb. Symp. Quant. Biol.* **42**, 1121-1135.
Penke, T. J. R., McKay, D. J., Strahl, B. D., Matera, A. G. and Duronio, R. J. (2016). Direct interrogation of the role of H3K9 in metazoan heterochromatin function. *Genes Dev.* **30**, 1866-1880.
Rangan, P., Malone, C. D., Navarro, C., Newbold, S. P., Hayes, P. S., Sachidanandam, R., Hannon, G. J. and Lehmann, R. (2011). piRNA production requires heterochromatin formation in Drosophila. *Curr. Biol.* **21**, 1373-1379.
Rea, S., Eisenhaber, F., O'Carroll, D., Strahl, B. D., Sun, Z.-W., Schmid, M., Opravil, S., Mechtler, K., Ponting, C. P., Allis, C. D. et al. (2000). Regulation of chromatin structure by site-specific histone H3 methyltransferases. *Nature* **406**, 593-599.
Riddle, N. C., Minoda, A., Kharchenko, P. V., Alekseyenko, A. A., Schwartz, Y. B., Tolstorukov, M. Y., Gorchakov, A. A., Jaffe, J. D., Kennedy, C., Linder-Basso, D. et al. (2011). Plasticity in patterns of histone modifications and chromosomal proteins in Drosophila heterochromatin. *Genome Res.* **21**, 147-163.
Rojas-Ríos, P., Chartier, A., Pierson, S. and Simonelig, M. (2017). Aubergine and piRNAs promote germline stem cell self-renewal by repressing the proto-oncogene Cbl. *EMBO J.* **36**, 3194-3211.
Rozhkov, N. V., Hammell, M. and Hannon, G. J. (2013). Multiple roles for Piwi in silencing Drosophila transposons. *Genes Dev.* **27**, 400-412.
Ryder, E., Blows, F., Ashburner, M., Bautista-Llacer, R., Coulson, D., Drummond, J., Webster, J., Gubb, D., Gunton, N., Johnson, G. et al. (2004). The DrosDel collection: a set of P-element insertions for generating custom chromosomal aberrations in Drosophila melanogaster. *Genetics* **167**, 797-813.

Saha, P., Sowpati, D. T. and Mishra, R. K. (2018). Epigenomic and genomic landscape of Drosophila melanogaster heterochromatic genes. *Genomics* (in press).
Sato, K. and Siomi, M. C. (2018). Two distinct transcriptional controls triggered by nuclear Piwi-piRISCs in the Drosophila piRNA pathway. *Curr. Opin. Struct. Biol.* **53**, 69-76.
Sato, M., Umetsu, D., Murakami, S., Yasugi, T. and Tabata, T. (2006). DWnt4 regulates the dorsoventral specificity of retinal projections in the Drosophila melanogaster visual system. *Nat. Neurosci.* **9**, 67-75.
Schulze, S. R., Sinclair, D. A. R., Fitzpatrick, K. A. and Honda, B. M. (2005). A genetic and molecular characterization of two proximal heterochromatic genes on chromosome 3 of Drosophila melanogaster. *Genetics* **169**, 2165-2177.
Sienski, G., Dönertas, D. and Brennecke, J. (2012). Transcriptional silencing of transposons by Piwi and maelstrom and its impact on chromatin state and gene expression. *Cell* **151**, 964-980.
Sienski, G., Batki, J., Senti, K.-A., Dönertas, D., Tirian, L., Meixner, K. and Brennecke, J. (2015). Silencio/CG9754 connects the Piwi-piRNA complex to the cellular heterochromatin machinery. *Genes Dev.* **29**, 2258-2271.
Smith, C. D., Shu, S., Mungall, C. J. and Karpen, G. H. (2007). The Release 5.1 annotation of Drosophila melanogaster heterochromatin. *Science* **316**, 1586-1591.
Smothers, J. F. and Henikoff, S. (2000). The HP1 chromo shadow domain binds a consensus peptide pentamer. *Curr. Biol.* **10**, 27-30.
Song, X., Zhu, C.-H., Doan, C. and Xie, T. (2002). Germline stem cells anchored by adherens junctions in the Drosophila ovary niches. *Science* **296**, 1855-1857.
Song, X., Wong, M. D., Kawase, E., Xi, R., Ding, B. C., McCarthy, J. J. and Xie, T. (2004). Bmp signals from niche cells directly repress transcription of a differentiation-promoting gene, bag of marbles, in germline stem cells in the Drosophila ovary. *Development* **131**, 1353-1364.
Strom, A. R., Emelyanov, A. V., Mir, M., Fyodorov, D. V., Darzacq, X. and Karpen, G. H. (2017). Phase separation drives heterochromatin domain formation. *Nature* **547**, 241-245.
Teo, R. Y. W., Anand, A., Sridhar, V., Okamura, K. and Kai, T. (2018). Heterochromatin protein 1a functions for piRNA biogenesis predominantly from pericentric and telomeric regions in Drosophila. *Nat. Commun.* **9**, 1735.
Thandapani, P., O'Connor, T. R., Bailey, T. L. and Richard, S. (2013). Defining the RGG/RG motif. *Mol. Cell* **50**, 613-623.
Tóth, K. F., Pezic, D., Stuwe, E. and Webster, A. (2016). The piRNA Pathway Guards the Germline Genome Against Transposable Elements. *Adv. Exp. Med. Biol.* **886**, 51-77.
Upadhyay, M., Martino Cortez, Y., Wong-Deyrup, S. W., Tavares, L., Schowalter, S., Flora, P., Hill, C., Nasrallah, M. A., Chittur, S. and Rangan, P. (2016). Transposon dysregulation modulates dWnt4 signaling to control germline stem cell differentiation in *Drosophila*. *PLoS Genet.* **12**, e1005918.
Van Doren, M., Williamson, A. L. and Lehmann, R. (1998). Regulation of zygotic gene expression in Drosophila primordial germ cells. *Curr. Biol.* **8**, 243-246.
Vanzo, N. F. and Ephrussi, A. (2002). Oskar anchoring restricts pole plasm formation to the posterior of the Drosophila oocyte. *Development* **129**, 3705-3714.
Wakimoto, B. T. and Hearn, M. G. (1990). The effects of chromosome rearrangements on the expression of heterochromatic genes in chromosome 2L of Drosophila melanogaster. *Genetics* **125**, 141-154.
Wang, S. H. and Elgin, S. C. R. (2011). Drosophila Piwi functions downstream of piRNA production mediating a chromatin-based transposon silencing mechanism in female germ line. *Proc. Natl. Acad. Sci. USA* **108**, 21164-21169.
Wang, X. and Page-McCaw, A. (2018). Wnt6 maintains anterior escort cells as an integral component of the germline stem cell niche. *Development* **145**, dev158527.
Wang, X., Pan, L., Wang, S., Zhou, J., McDowell, W., Park, J., Haug, J., Staehling, K., Tang, H. and Xie, T. (2011). Histone H3K9 trimethylase Eggless controls germline stem cell maintenance and differentiation. *PLoS Genet.* **7**, e1002426.
Wang, W., Han, B. W., Tipping, C., Ge, D. T., Zhang, Z., Weng, Z. and Zamore, P. D. (2015a). Slicing and binding by Ago3 or Aub trigger Piwi-bound piRNA production by distinct mechanisms. *Mol. Cell* **59**, 819-830.
Wang, S., Gao, Y., Song, X., Ma, X., Zhu, X., Mao, Y., Yang, Z., Ni, J., Li, H., Malanowski, K. E. et al. (2015b). Wnt signaling-mediated redox regulation maintains the germ line stem cell differentiation niche. *eLife* **4**, e08174.
Wang, J., Jia, S. T. and Jia, S. (2016). New Insights into the Regulation of Heterochromatin. *Trends Genet.* **32**, 284-294.
Wayne, S., Liggett, K., Pettus, J. and Nagoshi, R. N. (1995). Genetic characterization of small ovaries, a gene required in the soma for the development of the Drosophila ovary and the female germline. *Genetics* **139**, 1309-1320.
Wen, H., Andrejka, L., Ashton, J., Karess, R. and Lipsick, J. S. (2008). Epigenetic regulation of gene expression by Drosophila Myb and E2F2-RBF via the Myb-MuvB/dREAM complex. *Genes Dev.* **22**, 601-614.
Xie, T. and Spradling, A. C. (1998). decapentaplegic is essential for the maintenance and division of germline stem cells in the Drosophila ovary. *Cell* **94**, 251-260.
Yashiro, R., Murota, Y., Nishida, K. M., Yamashiro, H., Fujii, K., Ogai, A., Yamanaka, S., Negishi, L., Siomi, H. and Siomi, M. C. (2018). Piwi nuclear localization and its regulatory mechanism in drosophila ovarian somatic cells. *Cell Rep.* **23**, 3647-3657.
Yu, Y., Gu, J., Jin, Y., Luo, Y., Preall, J. B., Ma, J., Czech, B. and Hannon, G. J. (2015). Panoramix enforces piRNA-dependent cotranscriptional silencing. *Science* **350**, 339-342.
Zimyanin, V. L., Belaya, K., Pecreaux, J., Gilchrist, M. J., Clark, A., Davis, I. and St Johnston, D. (2008). In vivo imaging of oskar mRNA transport reveals the mechanism of posterior localization. *Cell* **134**, 843-853.

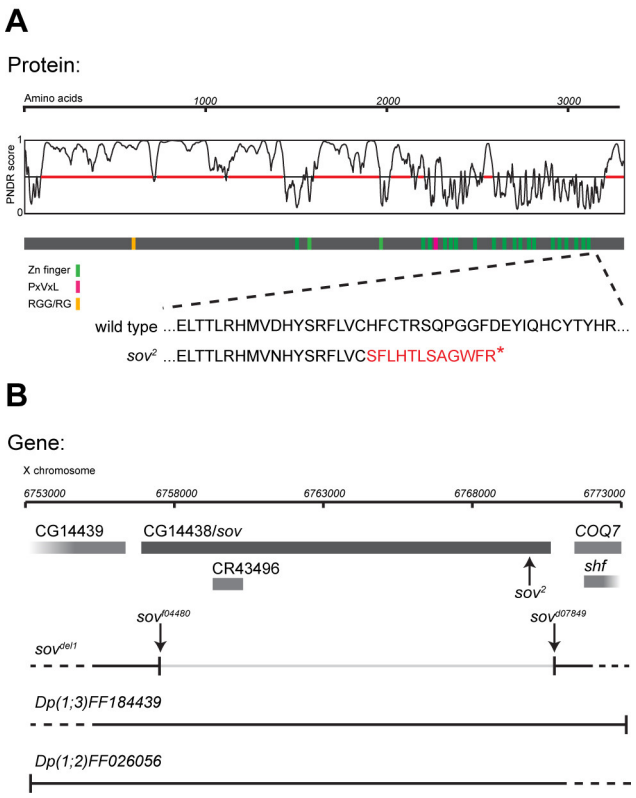

Figure S1. The Sov protein and the *sov*/CG14438 locus

(A) Domain composition and prediction of disordered regions of Sov protein is shown (Dunker et al., 2001). PNDR score >0.5 represents disorder and is indicated by red line. Alignment shows the wild type and *sov*^{2} mutant Sov protein sequences. Red letters indicate additional amino acids generated by a frame-shift mutation in *sov*^{2}.

(B) Schematic representation of the *sov* (CG14438) locus showing the mutant alleles used in this study.

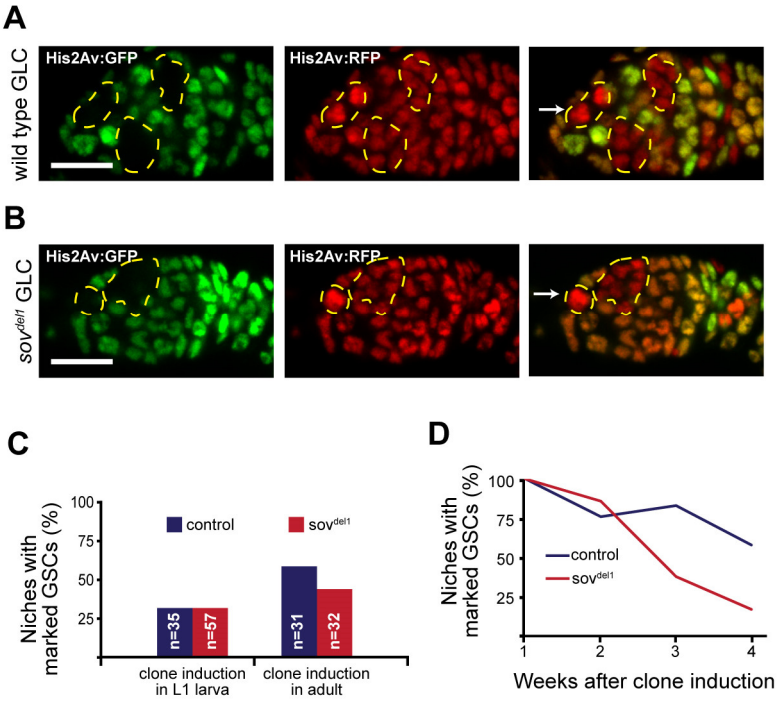

Figure S2. Analysis of germline clones (GLCs)

(A,B) Immunostaining of a germarium with a wild type (A) and *sov*^{del1} mutant (B) GLCs one week ACI. Heterozygous *sov*^{del1} mutant and control cells simultaneously express Histone2Av:RFP (red) and Histone2Av:GFP (green) and appear yellow on the merged image. Homozygous *sov*^{del1} mutant and wild type control GSCs have lost Histone2Av:GFP expression and appear red on the merged image (arrows). Yellow dashed lines outline the GLCs. Bars: 10 µm.

(C) The frequency of the induction of wild type and *sov*^{del1} homozygous mutant GLCs.

(D) Normalized frequency of germaria carrying wild type and *sov*^{del1} GLCs at various time points after clone induction. Sov mutant GSCs are progressively lost from the niche.

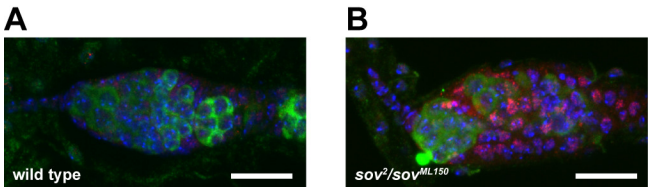

Figure S3. Caspase3 is activated in *sov* mutants

Apoptotic cells in wild type (A) and sov^{2}/sov^{ML150} (B) mutant germaria were labeled with cleaved Caspase3 (red). Activated Caspase3 accumulates in the *sov* mutant niches. Germ cells are labelled with Vasa (green), DAPI is blue. Scale bars: 10 μm.

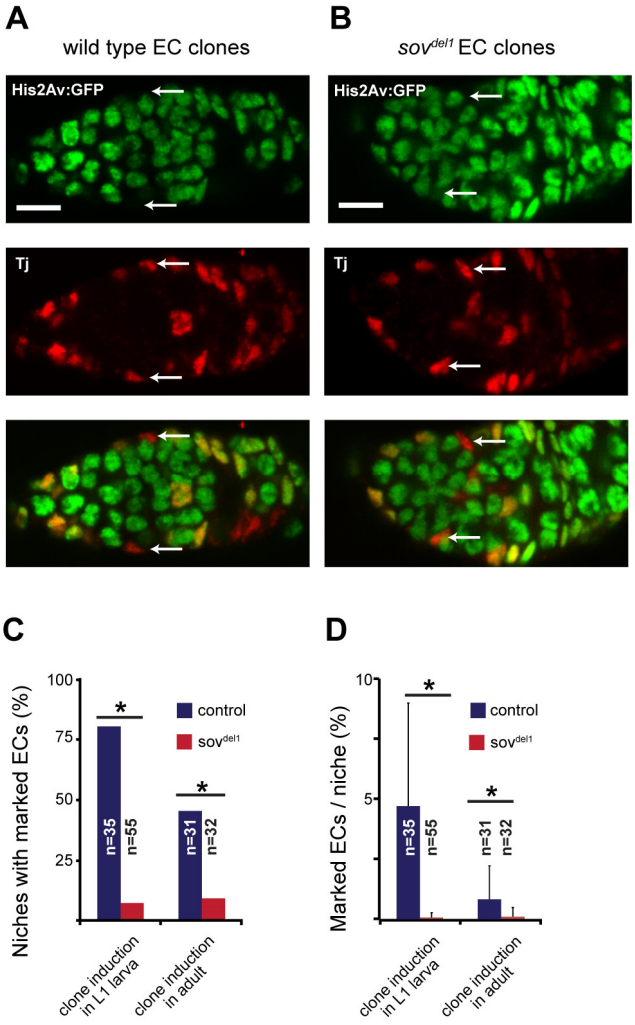

Figure S4. Analysis of EC clones

(A,B) Immunostaining of a germarium with wild type (A) and *sov*^{del1} mutant (B) EC clones three days ACI. Heterozygous cells ubiquitously express Histone2Av:GFP (green). Somatic cells were labelled with Tj (red). Homozygous *sov*^{del1} mutant and wild type control ECs have lost Histone2Av:GFP expression and appear red on the merged image (arrows). Bars: 10 µm.

(C,D) Frequency (C) and size (D) of wild type and *sov*^{del1} EC clones in four-day old females. The reduced clone frequency and clone size indicates a requirement for *sov* in EC survival. Mean±s.d. is shown, T-test, * $p<0.05$.

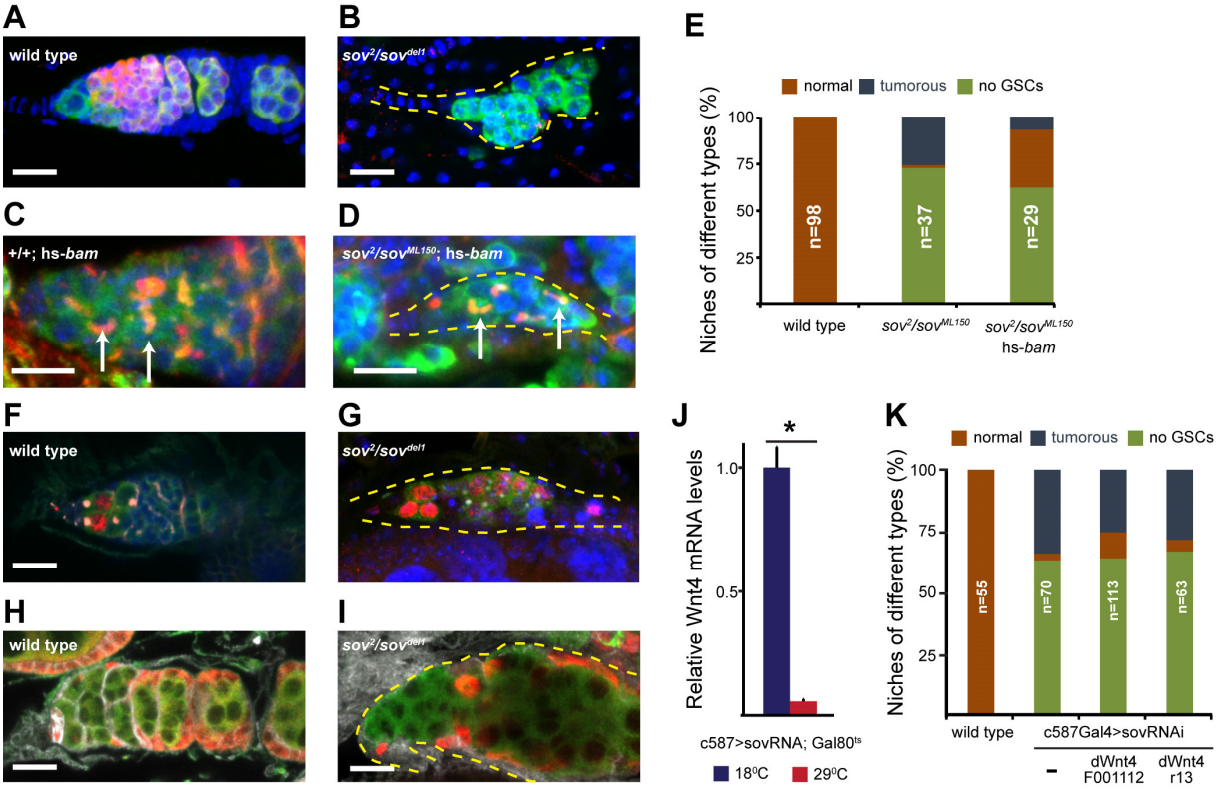

Figure S5. Sov promotes GSC differentiation by restricting dpp-signalling activity in the niche

(A,B) Immunostaining of a wild type germarium expressing *bam*>GFP (A), and a tumorous sov^{2}/sov^{del1} germarium (B) with no detectable *bam*>GFP expression. Germ cells are labelled with Vasa (green), bam>GFP is red, DAPI is blue. Yellow dashed line outlines the germarium in (B). Bars: 10µm.

(C,D) Immunostaining of a germaria of +/+;hs-*bam* (C) and sov^{2}/sov^{ML150}; hs-*bam* (D) females. White arrows indicate fusomes. Forced expression of *bam* induces the differentiation of the *sov* mutant germ cells. Spectrosomes and fusomes are labelled with HTS (red), germ cells are labelled with Vasa (green), DAPI is blue. Yellow dashed line outlines the germarium in (D). Bars: 10µm.

(E) Quantification of the mutant niche phenotypes. *Sov* acts upstream of *bam* in the GSC differentiation process.

(F,G) Immunostaining of a wild type germarium (F) and a sov^{2}/sov^{del1} germarium (G). Spectrosomes and fusomes are labelled with HTS (white), germ cells are labelled with Vasa (green), germ cells responding to Dpp signal are labelled with pMad (red), DAPI is blue. Bars: 10µm

(H,I) Immunostaining of a wild type (H) and a sov^{2}/sov^{del1} germaria (I). Germ cells are labelled with Vasa (green). Somatic cells are labelled with Tj (red). Protrusions are labelled with Coracle (white). *Sov* mutant ECs fail to extend protrusions. Bars: 10µm.

(J) RT-qPCR measurement of mRNA levels of Wnt4. For the analysis, *c587Gal4; Gal80^{ts}/sovRNAi* females were shifted from 18ºC to 29ºC and their ovaries were used. Control flies were kept at 18ºC. Mean±s.d. is shown, T-test, * $p<0.05$.

(K) Quantification of the mutant niche phenotypes.

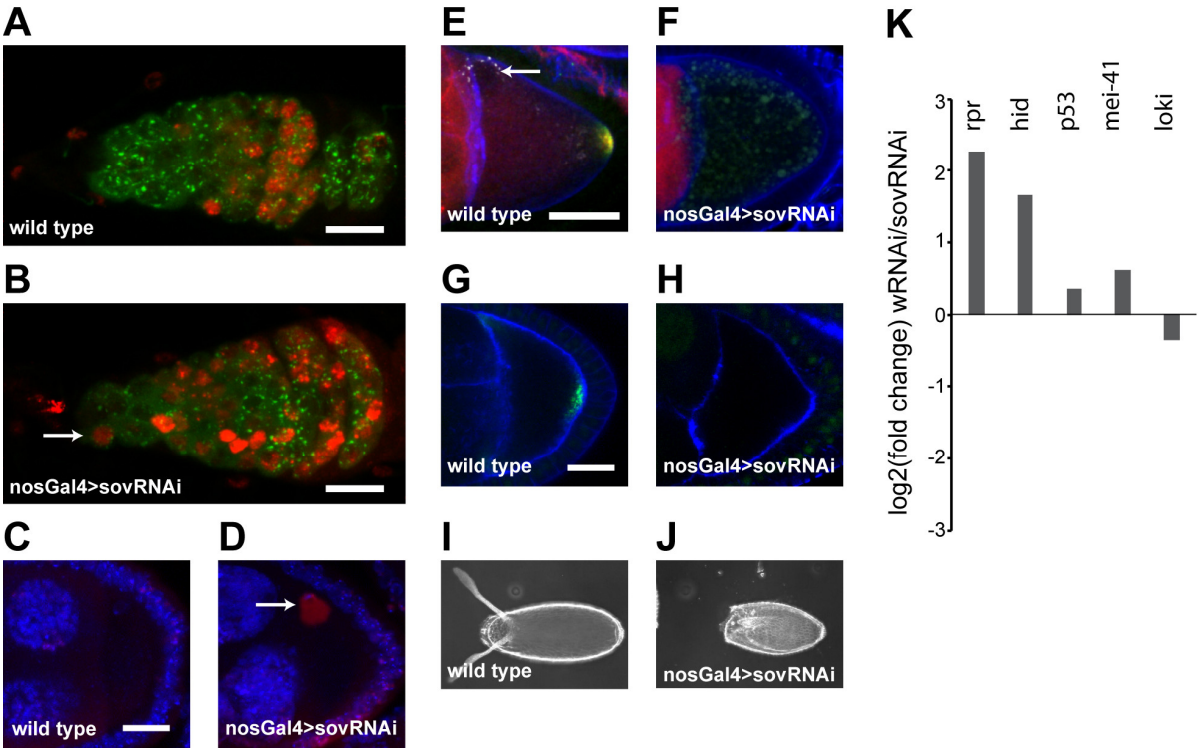

Figure S6. Loss of *sov* induces DNA damage, abnormal axis specification and apoptosis in the germ line

(A-H) Immunostaining of ovaries of wild type (A,C,E,G) and nosGal4>*sov*RNAi (B,D,F,H) females. (A-B) Germ cells are labelled with Vasa (green). (A,B) Double-strand breaks are labelled with γH2Av (red), germ cells are labelled with vasa (green), DAPI is blue. Arrow indicates a GSC expressing γH2Av. Scale bar: 10µm.(C,D) Shown are oocytes. Double-strand breaks are labelled with γH2Av (red), DAPI is blue. Arrow indicates the nucleus of a *sov* silenced oocyte accumulating γH2Av. (E,F) Vasa (green) and Osk (red) colocalize at the posterior pole, Grk (white, indicated by an arrow) localizes at the anterodorsal corner of the oocyte. The outline of the oocyte is labelled by actin staining (blue) Scale bar: 20µm. (G,H) *osk* mRNA is visualized by *MS2:GFP/oskMS2* (green). The outline of the oocyte is labelled by actin staining (blue) Scale bar: 10µm.

(I,J) Displayed are eggs laid by wild type (I) and *nosGal4>sovRNAi* (J) females.

(K) Expression of genes regulating apoptosis. Expression of *rpr* and *hid* is upregulated in nosGal4>*sov*RNAi ovaries.

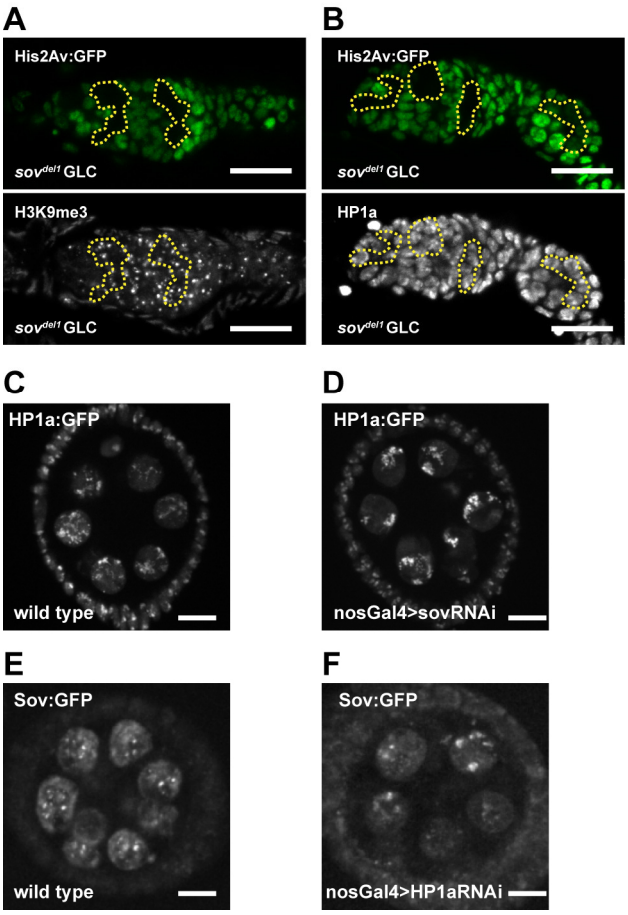

Figure S7. Sov is dispensable for H3K9me3 and HP1a localization

(A,B) Immunostaining of germaria with *sov*^{del1} mutant GLCs. Scale bars: 10 µm. GLCs are negatively marked by the lack of Histone2Av:GFP signal (green). *Sov*^{del1} mutant GLCs are outlined by dotted line. H3K9me3 (A) and HP1a (B) are labelled white.

(C-F) Displayed are wild type (C,E) *sov*-silenced (D) and HP1a-silenced (F) living egg chambers. Egg chambers express HP1a:GFP (C,D) and Sov:GFP (E,F) Scale bars: 10µm.

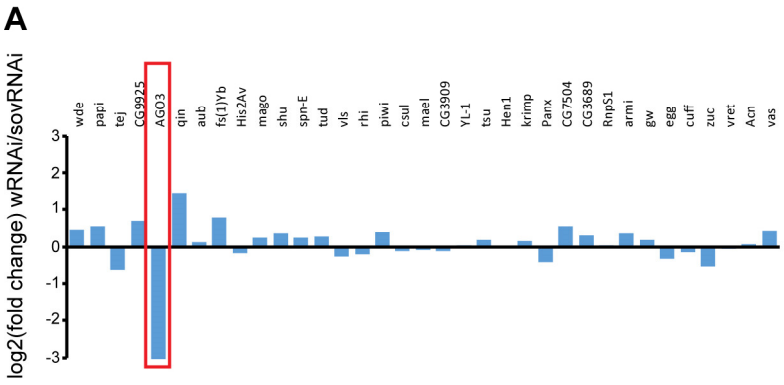

Figure S8. Sov regulates expression of *Ago3*

(A) Expression of genes involved in the piRNA-pathway. *Ago3* expression is reduced in *nosGal4>sovRNAi* ovaries.

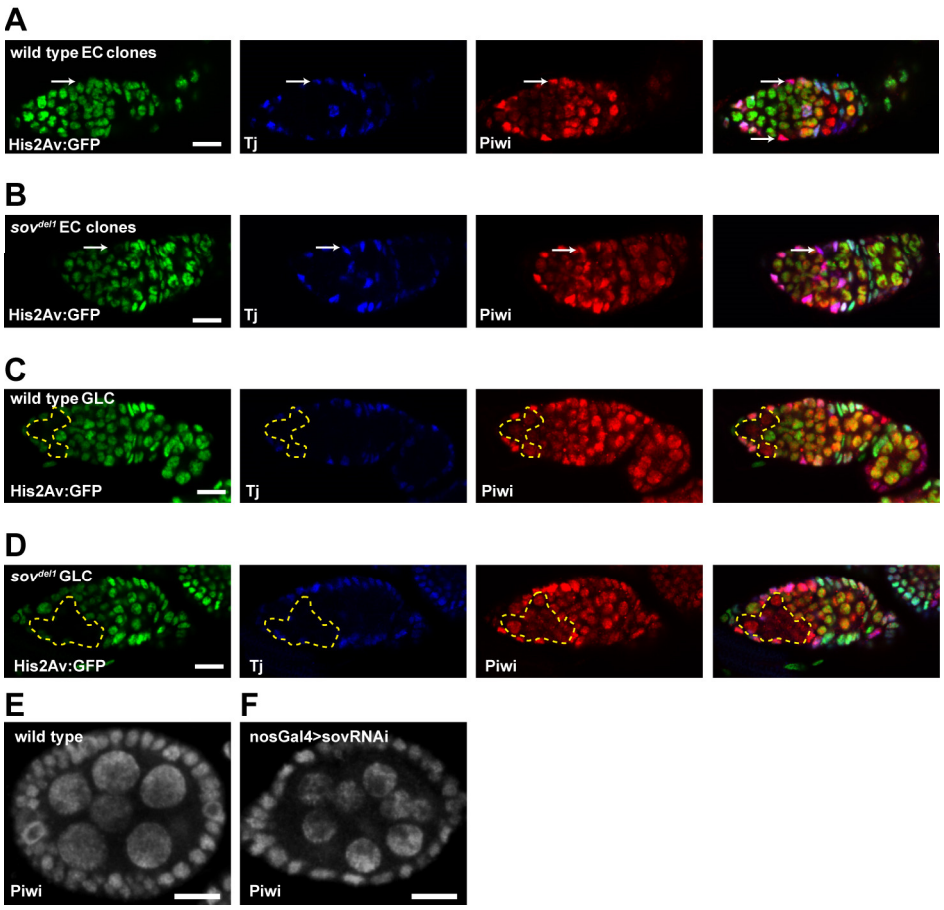

Figure S9. Sov is dispensable for nuclear localization of Piwi

(A-D). Immunostaining of germaria carrying wild type (A,C) and *sov*^{del1} mutant (B,D) EC clones and GLCs. Clones are negatively marked by the lack of Histone2Av:GFP signal (green). GLCs are outlined by dotted line, arrows mark EC clones. Tj is labelled blue, Piwi is labelled red. In the *sov* mutant germ cells and ECs, Piwi is localized in the nuclei. Bars:10 µm.

(E,F) Immunostaining of wild type (E) and *nosGal4>sovRNAi* (F) egg chambers. Piwi is labelled white. In the *sov*-silenced germ cells, Piwi is localized in the nuclei.

Table S1. List of primary antibodies

Antigene	Host	Dilution	Reference
Tj	guinea pig	1:10000	(Li et al., 2003)
vasa	rat	1:300	DSHB
Hts	mouse	1:20	1B1, DSHB
Coracle	mouse	1:200	C615.16, DSHB
Rhino	guinea pig	1:2000	(Klattenhoff et al., 2009)
Piwi	rabbit	1:1000	(Klattenhoff et al., 2009)
Gurken	mouse	1:10	1D12, DSHB
H3K9me3	rabbit	1:100	ab8898, Abcam
Oskar	rabbit	1:2000	(Vanzo and Ephrussi, 2002)
Gamma-H2Av	mouse	1:50	UNC93-5.2.1, DSHB
HP1a	mouse	1:50	C1A9, DSHB
cleaved-Caspase3	rabbit	1:200	5A1E, Cell Signalling
Fas3	mouse	1:25	7G10, DSHB

Table S2. List of primers used for RT-qPCR.

Primer	Sequence
cl1-A-rt-plus	CGAAGCCTTAGATCTCGCTCC
cl1-A-rt-minus	ACATCAGGAACACAGCGAGGTG
cl2-A-rt-plus	GTGCCGGAGCGTGGGTCCAG
cl2-A-rt-minus	GGTGACATGAAAATCGCATC
flam-rt-plus	GCAATAGTACGCTAGTCCG
flam-rt-minus	GGCTATGAGGATCAGACAG
rp49-rt	GGAGGAGACGCCG
cl1-A-f	CGTCCCAGCCTACCTAGTCA
cl1-A-r	ACTTCCCGGTGAAGACTCCT
cl2-A-f	GCCTACGCAGAGGCCTAAGT
cl2-A-r	CAGATGTGGTCCAGTTGTGC
flam-f	TGAGGAATGAATCGCTTTGAA
flam-r	TGGTGAAATACCAAAGTCTTGGGTCAAC
rp49-f	CCGCTTCAAGGGACAGTATCTG
rp49-r	ATCTCGCCGCAGTAAACGC
Wnt4-f	AAGCAGCGACGCAAGAAACC
Wnt4-r	CCACAGTTGTCCGGATGCAG
HeT-A-f	CGCGCGGAACCCATCTTCAGA
HeT-A-r	CGCCGCAGTCGTTTGGTGAGT
Burdock-f	CGGTAAAATCGCTTCATGGT
Burdock-r	ACGTTGCATTTCCCTGTTTC
gypsy-f	GTTCATACCCTTGGTAGTAGC
gypsy-r	CAACTTACGCATATGTGAGT
GFP-f	GATCACTCTCGGCATGGACG
GFP-r	AAGGAATTTGCTTTACCGCTATGA

Movie 1

Frap analysis of HP1a. Movie showing recovery of HP1a:EGFP fluorescence in wild-type and *nosGal4*>sovRNAi nuclei in a representative FRAP experiment.